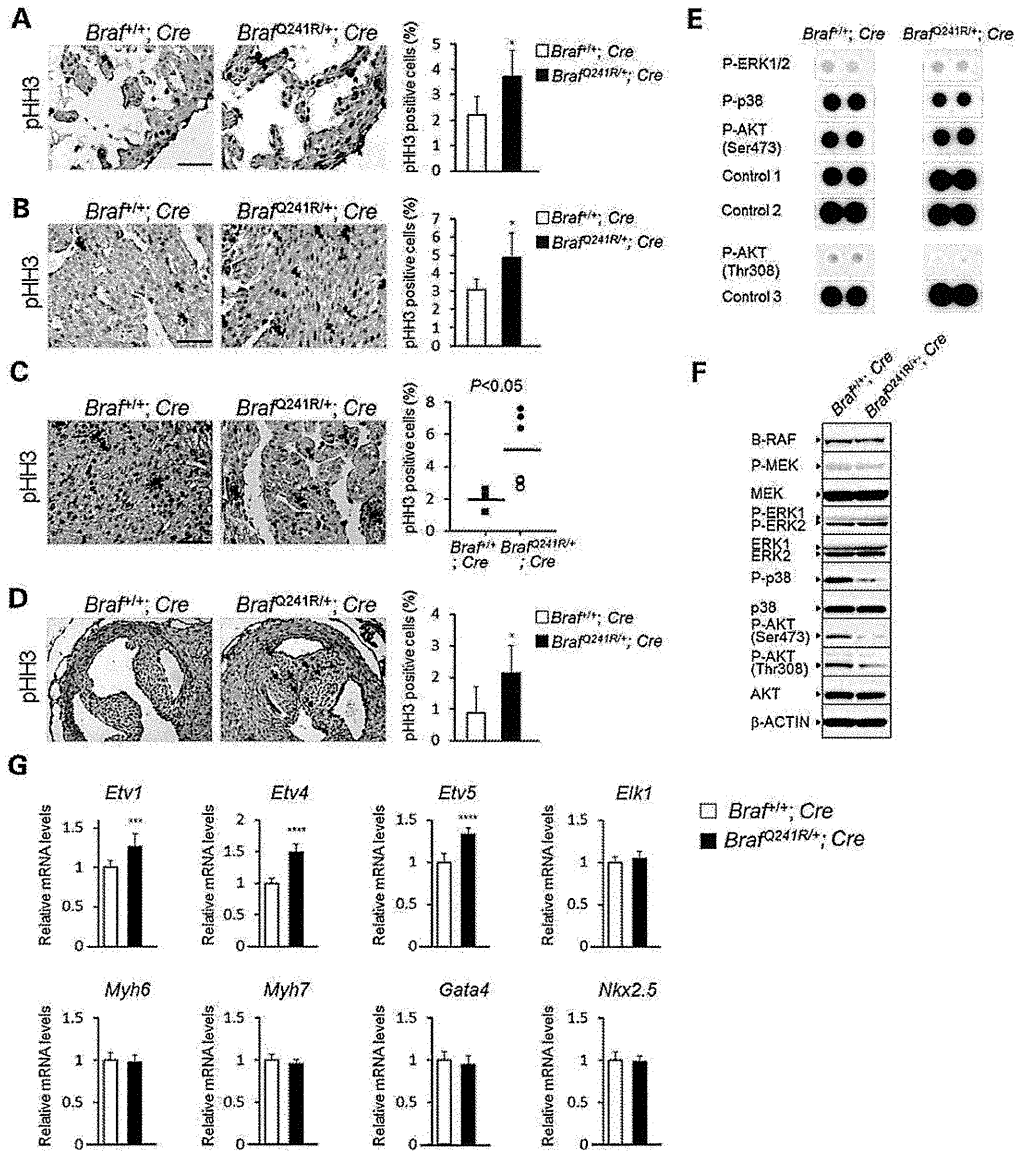

Figure 4. Increased cell proliferation and altered multiple signaling pathways in *Braf*$^{Q241R/+}$; *Cre* embryo hearts. (**A**–**D**) Immunostaining for pHH3 in the myocardium (A), interventricular septum (B and C) and pulmonary valves (D) of *Braf*$^{+/+}$; *Cre* and *Braf*$^{Q241R/+}$; *Cre* embryos at E13.5 (A and B) and E16.5 (C and D). The arrows indicate representative positive cells. *Braf*$^{Q241R/+}$; *Cre* embryos with or without VSD are shown in closed cycles or open circles, respectively. Scale bars 50 μm (A–C). Data are means ± SD (A and B) *Braf*$^{+/+}$; *Cre* ($n = 5$) and *Braf*$^{Q241R/+}$; *Cre* ($n = 5$). (C and D) *Braf*$^{+/+}$; *Cre* ($n = 3$) and *Braf*$^{Q241R/+}$; *Cre* ($n = 6$). $^{*}P < 0.05$ versus *Braf*$^{+/+}$; *Cre*. (**E**) Protein extracts (400 μg) of the hearts from *Braf*$^{+/+}$; *Cre* and *Braf*$^{Q241R/+}$; *Cre* embryos at E16.5 were subjected to Phospho-Kinase Antibody Array. Results are representative of gene spots that showed significant changes in 45 phosphorylated proteins. (**F**) Western blotting of the hearts from *Braf*$^{+/+}$; *Cre* and *Braf*$^{Q241R/+}$; *Cre* embryos at E16.5 (pooled samples; *Braf*$^{+/+}$; *Cre* ($n = 5$), *Braf*$^{Q241R/+}$; *Cre* ($n = 5$)). β-Actin is shown as a loading control. The arrowheads indicate the bands corresponding to each protein. (**G**) Cardiac mRNA levels were determined by quantitative reverse transcription–PCR. mRNA levels were normalized by those of *Gapdh*, and those in *Braf*$^{+/+}$; *Cre* at E18.5 are set at 1. Data are the means ± SD (*Braf*$^{+/+}$; *Cre* ($n = 10$) and *Braf*$^{Q241R/+}$; *Cre* ($n = 6$)). $^{***}P < 0.001$, $^{****}P < 0.0001$ versus *Braf*$^{+/+}$; *Cre*. *Etv1*, *Etv4*, *Etv5*, *Myh6* and *Myh7* encode ER81, Pea3, ERM, α-MHC and β-MHC, respectively.

prenatal treatment of PD0325901 (1.0 mg/kg) (7 of 37, $P = 0.32$, χ^2 test for deviation from the Mendelian ratios). PD0325901-treated *Braf*$^{Q241R/+}$; *Cre* embryos appeared normal without edema and mandibular hypoplasia (0 of 31 at E16.5 to P0), whereas other genotype mice, excluding *Braf*$^{Q241R/+}$; *Cre* treated with PD0325901, showed teratogenic effects, including open eyes (Supplementary Material, Fig. S9), edema, enlarged semilunar valves and atrioventricular valves (data not shown). Other compounds had no effect on the recovery of embryonic lethality in *Braf*$^{Q241R/+}$; *Cre* embryos.

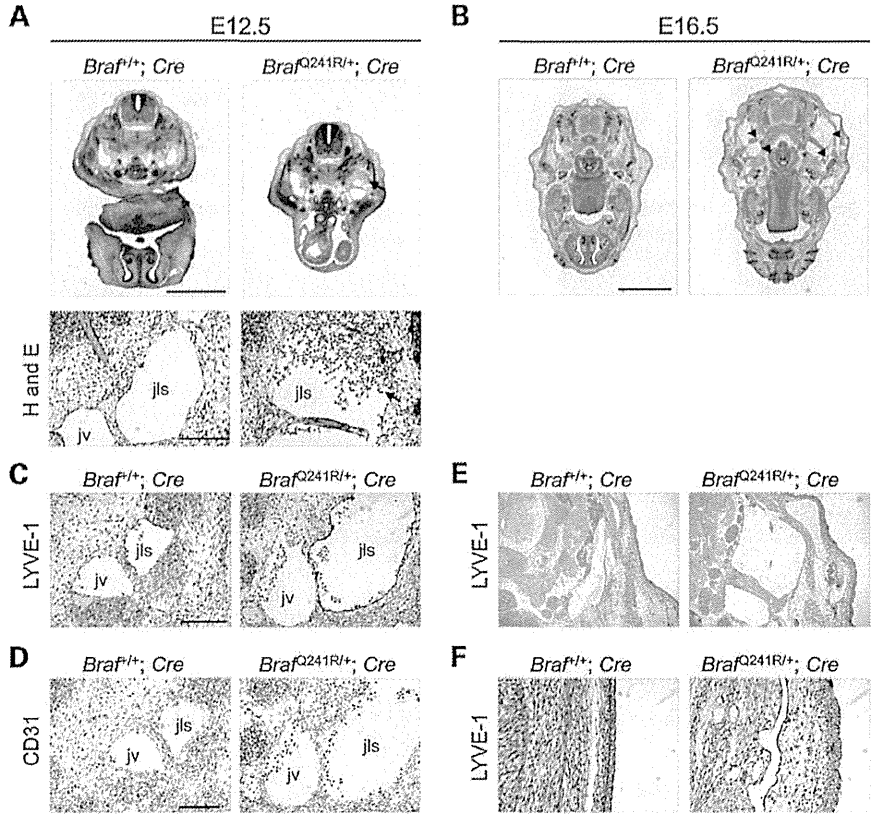

Figure 5. Abnormal lymphatic development in $Braf^{Q241R/+}$; *Cre* embryos. (**A** and **B**) Transverse sections of $Braf^{+/+}$; *Cre* and $Braf^{Q241R/+}$; *Cre* embryos at E12.5 (A) and E16.5 (B) stained with H&E. Lower panels show high-magnification views of jugular lymph sac (A). The arrows (A) and arrowheads (B) indicate blood cells in jugular lymph sacs and the regions which are similar to the jugular lymph sacs or jugular veins of embryos at E12.5, respectively. Scale bars 1 mm (in upper panels, A), 100 μm (in lower panels, A) and 2 mm (B). (**C–F**) Sections of $Braf^{+/+}$; *Cre* and $Braf^{Q241R/+}$; *Cre* embryos at E12.5 (C and D) and E16.5 (E and F) stained with antibodies against lymphatic endothelial markers, LYVE-1 (C, E and F) or CD31 (D). (F) Subcutaneous lymphatic vessels. jls, jugular lymph sac; jv, jugular vein.

Thus, PD0325901 treatment prevented embryonic lethality in $Braf^{Q241R/+}$; *Cre* embryos and could ameliorate edema and mandibular hypoplasia.

Epigenetic regulation of gene expression, such as histone acetylation and histone methylation, plays a crucial role in the transcriptional regulation of cell differentiation, development, the inflammatory response and cancer (25). Recently, a histone deacetylase inhibitor, SAHA [vorinostat (Zolinza)], has been used in the treatment of lymphomas and solid tumors. Recent studies have suggested the association of UTX and JMJD3, a histone H3 lysine 27 (H3K27) demethylase, with heart development (26–28). We therefore tested whether treatment using these compounds leads to the rescue of embryonic lethality (Table 2). SAHA treatment had no effect (data not shown); however, one embryo survived for 3 weeks with prenatal treatment of GSK-J4 (inhibitors of histone H3K27 demethylase UTX and JMJD3; 5.0 mg/kg) (25) or NCDM-32b (inhibitor of histone H3K9 demethylase JMJD2C; 5.0 mg/kg) (29). Moreover, co-treatment with GSK-J4 (5.0 mg/kg) and PD0325901 (0.5 mg/kg) further increased the number of $Braf^{Q241R/+}$; *Cre* mice alive at weaning (5 of 31, $P = 0.14$). The teratogenic effects, which were frequently observed in PD0325901 treatment, were not observed in the co-treatment with GSK-J4 and PD0325901.

We further investigated whether co-treatment with PD0325901 and GSK-J4 prevented heart defects in $Braf^{Q241R/+}$; *Cre* embryos. Co-treatment with PD0325901 and GSK-J4, but not PD0325901 treatment (1.0 mg/kg) alone, ameliorated enlarged pulmonary, tricuspid and mitral valves in $Braf^{Q241R/+}$; *Cre* embryos (Fig. 6A and B). However, no difference in the frequency of heart defects, including VSD, hypertrabeculation, epicardial blisters and noncompaction, was observed. It is noteworthy that treatment with PD0325901 or GSK-J4 alone or the co-treatment reversed the decrease of phosphorylated p38 protein levels (Fig. 6C; Supplementary Material, Fig. S10). These results suggest that combination treatment with PD0325901 and GSK-J4 prevents embryonic lethality, enlarged cardiac valves and decreased phosphorylated p38 in $Braf^{Q241R/+}$; *Cre* embryos.

DISCUSSION

In this study, we generated heterozygous *Braf* Q241R-expressing mice, which exhibited embryonic and postnatal lethality due to liver necrosis, skeletal abnormalities, lymphatic defects and various cardiac defects, including cardiomegaly, noncompaction, enlarged cardiac valves and hypertrabeculation.

Table 2. Rescue of embryonic lethality in *Braf*$^{Q241R/+}$; *Cre* embryos by MEK inhibitor, histone demethylase inhibitor or these combined treatment

Compound	Dose (mg/kg body weight)	Genotype (3 weeks) *Braf*$^{+/+}$	*Braf*$^{+/+}$; *Cre*	*Braf*$^{Q241R\ Neo/+}$	*Braf*$^{Q241R/+}$; *Cre*	n^a	n^b	n^c	*P*
DMSO (vehicle)	–	14	8	8	0	30	6	5.0	<0.01
PD0325901	0.5	7	14	7	2	30	13	2.3	0.02
	1.0	11	13	6	7	37	14	2.6	0.32
MAZ51	1.0	9	8	11	0	28	6	4.7	0.02
	2.0	10	14	7	0	31	6	5.2	<0.01
	5.0	10	7	11	0	28	11	2.5	0.01
Sorafenib	5.0	12	15	8	0	35	13	2.7	<0.01
Lovastatin	5.0	8	19	17	0	44	10	4.4	<0.01
Everolimus	0.1	6	6	9	0	21	9	2.3	0.04
NCDM-32b	2.0	12	4	9	0	25	9	2.8	<0.01
	5.0	10	10	14	1	35	11	3.2	0.02
	10.0	11	10	19	0	40	9	4.4	<0.01
GSK-J4	5.0	8	18	14	1	41	11	3.7	<0.01
	10.0	16	26	20	0	62	23	2.7	<0.01
PD0325901 + GSK-J4	0.5 + 5.0	8	13	5	5	31	10	3.1	0.14

Male *Braf*$^{Q241R\ Neo/+}$ mice were crossed with female *Braf*$^{+/+}$; *Cre* mice, and pregnant mice were intraperitoneally injected with vehicle or various compounds shown daily from E10.5 to E18.5. Deviation from the expected Mendelian ratios was assessed by χ^2 test. n^a, the total number of acquired pups. n^b, the total number of treated female *Braf*$^{+/+}$; *Cre* mice. n^c, the average number of survived pups at weaning (n^a/n^b).

Increased expression of Ets transcription factors and decreased expression of cardiac phosphorylated p38 in embryonic heart tissues were observed. PD0325901 treatment, in part, rescued embryonic and postnatal lethality in *Braf*$^{Q241R/+}$; *Cre* mice. One pup in *Braf*$^{Q241R/+}$; *Cre* also survived until P21 with treatment of GSK-J4 or NCDM-32b. PD0325901 treatment, but not GSK-J4 and NCDM-32b treatment, ameliorated edema and mandibular hypoplasia. Moreover, PD0325901 co-treatment with GSK-J4 further rescued embryonic lethality with recovered hypertrophy of pulmonary, tricuspid and mitral valves and the decreased expression of phosphorylated p38. Taken together, mice expressing a development-specific *Braf* Q241R mutation will be useful to further clarify the pathogenesis of CFC syndrome and to develop therapeutic approaches.

Patients with RASopathies are characterized by generalized abnormalities of lymphatic development. Fetuses with RASopathies have been shown to be characterized by hydrops, pleural effusions, increased nuchal translucency due to distended JLS and cystic hygroma in utero (30–32). Children and adults with RASopathies show generalized lymphedema, peripheral lymphoedema or pulmonary lymphangiectasia (33). Our new model, *Braf*$^{Q241R/+}$; *Cre* mice, showed embryonic and postnatal lethality and exhibited multiple developmental defects in the lymphatic system, including hydrops, distended JLS and subcutaneous lymphatic vessels. In contrast, mice of other knockin mouse models for RASopathies survived to adulthood and have not shown the defects in lymphatic system (34–36). Thus, for the first time our new model *Braf*$^{Q241R/+}$; *Cre* mice demonstrated the developmental lymphatic defects, which are the common features observed in RASopathies, in knockin mouse models for RASopathies.

Dysregulation of the RAS–MAPK pathway is a common underlying mechanism of RASopathies. However, a variety of compounds, including the RAS–MAPK pathway and other signaling pathways, has been effective for ameliorating the defects in previous knockin mouse models of RASopathies. MEK inhibitors have been found to ameliorate the cardiac defects and skeletal features in mice expressing *SOS1* and *RAF1* mutations (24,35). Angiotensin II inhibitor ameliorates the phenotypes of hypertension, vascular remodeling and fibrosis of the kidney and heart in mice expressing *HRAS* G12V mutation (36), and mTOR inhibitor ameliorates hypertrophic cardiomyopathy in a mouse model of LEOPARD syndrome, expressing a catalytically inactive mutation in SHP2 (34). We examined a variety of compounds, including anti-cancer agents, MEK inhibitor, mTOR inhibitor, VEGFR3 inhibitor, BRAF inhibitor and farnesyl transferase inhibitor using our *Braf*$^{Q241R/+}$; *Cre* mice. Treatment with MEK inhibitor, but not mTOR inhibitor, in *Braf*$^{Q241R/+}$; *Cre* mice ameliorated embryonic lethality and skeletal abnormalities, suggesting that the pathogenesis of the disease is similar to those in *SOS1* and *RAF1* mutations. Thus, our new *Braf*$^{Q241R/+}$; *Cre* mice will be useful to screen various compounds for therapeutic approaches to RASopathies.

The exact mechanisms by which the single treatment of histone demethylase inhibitor or co-treatment of MEK inhibitor and histone demethylase inhibitor were effective for *Braf*$^{Q241R/+}$; *Cre* mice have not yet been characterized. Lysine modification of histone 3, acetylation and methylation, is associated with gene activation or silencing (37). In gene expression, inactive genes show methylation at lysine 27, and permanently silenced genes frequently are characterized by methylation at lysine 9 (37). Histone H3K27 methylase, *Ezh2*, conditional knockout mice in cardiomyocytes have been reported to show abnormal heart development, such as noncompaction and excessive trabeculation (38). Meanwhile, deletion of histone H3K27 demethylase, UTX, has been identified in individuals with Kabuki syndrome, who showed distinctive facial appearance and congenital heart disease (39). H3K9 methyltransferases, G9a and GLP, have been shown to be essential for cardiac morphogenesis (40). It is of note that the balance between methylation and demethylation of H3 is required for normal cardiac differentiation. *De novo* mutations in *SMAD2*, a transcription factor which regulates H3K27 methylation in embryonic left–right organizer, have been identified in children with congenital heart disease (28). *SMAD2*, which is regulated by ERK (41), has been found to bind to H3K27 demethylase JMJD3, and regulate H3K27 methylation

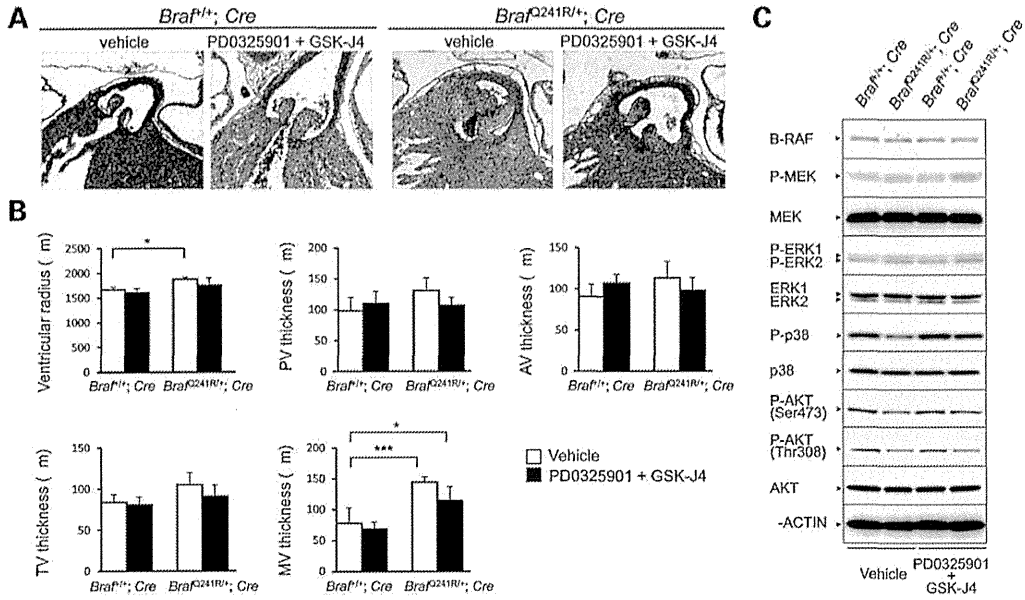

Figure 6. Influence of co-treatment with PD0325901 and GSK-J4 on the cardiac phenotype and signaling of *Braf*$^{Q241R/+}$; *Cre* embryos. (**A** and **B**) Sequential sections of embryonic hearts from *Braf*$^{+/+}$; *Cre* and *Braf*$^{Q241R/+}$; *Cre* at E16.5 stained H&E. (A) Histological sections of pulmonary valves. (B) The ventricular radius and the thicknesses of the cardiac valve leaflets were measured at their largest diameter in serial sections. Data are means ± SD (vehicle; *Braf*$^{+/+}$; *Cre* ($n = 5$), *Braf*$^{Q241R/+}$; *Cre* ($n = 5$). PD0325901 + GSK-J4; *Braf*$^{+/+}$; *Cre* ($n = 7$), *Braf*$^{Q241R/+}$; *Cre* ($n = 11$)). $^{*}P < 0.05$, $^{***}P < 0.001$ (Tukey–Kramer test). NS, not significant. (**C**) Western blotting of the hearts from *Braf*$^{+/+}$; *Cre* and *Braf*$^{Q241R/+}$; *Cre* embryos at E16.5 (vehicle-treated pooled samples; *Braf*$^{+/+}$; *Cre* ($n = 8$), *Braf*$^{Q241R/+}$; *Cre* ($n = 8$). PD0325901 + GSK-J4-treated pooled samples; *Braf*$^{+/+}$; *Cre* ($n = 8$), *Braf*$^{Q241R/+}$; *Cre* ($n = 7$)). β-Actin is shown as a loading control. The arrowheads indicate the bands corresponding to each protein.

(28), suggesting that the histone demethylase JMJD3 is associated with heart development in humans by indirect regulation of ERK. In addition, constitutively activated BRAF and RAS mutants, through ERK activation, have been shown to induce JMJD3 and EZH2 expression (42,43). These observations suggest that activation of BRAF or ERK is associated with histone H3K27 modification, regulating cardiac development. In this study, the total content of the H3K27me3 in heart tissues of *Braf*$^{Q241R/+}$; *Cre* or *Braf*$^{Q241R/+}$; *Cre* mice after GSK-J4 co-treatment with PD0325901 was comparable with that of *Braf*$^{+/+}$; *Cre* mice (data not shown). Furthermore, the histone H3K27 demethylase activity of lysates from *Braf*$^{Q241R/+}$; *Cre* embryos at E14.5 was comparable with that of *Braf*$^{+/+}$; *Cre* (data not shown). Further analysis of H3K9 and H3K27 modification status on individual genes will clarify the mechanism by which histone demethylase inhibitor is effective against embryonic and postnatal lethality and developmental defects in *Braf*$^{Q241R/+}$; *Cre* mice.

MEK inhibitor treatment or crossing with ERK1 knockout mice has improved the hypertrophy of cardiac valves in Noonan syndrome model mice with a *SOS1* or *PTPN11* mutation (24,44). In contrast, treatment of MEK inhibitor did not lead to the amelioration of enlarged cardiac valves in *Braf*$^{Q241R/+}$; *Cre* embryos. Furthermore, other mice, excluding *Braf*$^{Q241R/+}$; *Cre*, treated with MEK inhibitor showed enlarged cardiac valves (data not shown), suggesting that the vital nature of MEK/ERK signaling balance in cardiac valve development. Given that no MEK inhibitor activity nor the inhibition activity of other protein kinases has been reported in GSK-J1 (GSK-J4 sodium salt) (25), these results suggest that not only MEK/ERK signaling balance but also histone H3K27 modification can play a crucial role in the normal development of cardiac valve in *Braf*$^{Q241R/+}$; *Cre* embryos.

The natural history and the frequency of tumors in adult CFC patients have not been fully elucidated (6). Since molecular analysis became available, three individuals with *BRAF* mutation have been reported to have developed acute lymphoblastic leukemia and non-Hodgkin lymphoma (6). Knockin mice expressing *BRAF* L597V mutation survived to adulthood and showed multiple Noonan syndrome/CFC syndrome phenotypes, including short stature, facial dysmorphia and cardiac enlargement (12). The L597V is located in the CR3 kinase domain and leads to 2-fold elevated BRAF kinase activity (45). The L597V mutation has been identified in 11 somatic cancers (COSMIC; http://cancer.sanger.ac.uk/cancergenome/projects/cosmic/) and three patients with Noonan syndrome (13,46,47), which generally shows milder phenotype than that in CFC syndrome. In contrast, Q257R mutation is located in the CR1 domain and has been identified in 40% of CFC syndrome, not in cancers. Our ELK transactivation study has shown that level of ELK transactivation in Q257R was a half of V600E (3). The previous report showed that BRAF Q257R has increased BRAF kinase activity compared with WT and the activity was as high as that of the V600E (4). It is possible that differences in kinase activity and/or the effect on downstream pathways could cause the phenotypic differences in these knockin mice. Surviving *Braf*$^{Q241R/+}$; *Cre* mice in the PD0325901 treatment showed distinctive facial appearance, abnormal dental occlusion, reduced postnatal length and weight, kyphosis and skin

disease, which are similar to CFC syndrome phenotype (data not shown) (1,48). *Braf*$^{Q241R/+}$; *Cre* mice also survived to adulthood when these mice (C57BL/6J background) were crossed with ICR or BALB/c mice (unpublished data). Further studies will be necessary to examine if adult *Braf*$^{Q241R/+}$; *Cre* mice show phenotypes similar to patients with CFC syndrome, including seizures and tumor development.

The potential mechanism of activation and downregulation of multiple signaling pathways in *Braf*$^{Q241R/+}$; *Cre* embryos is unclear. In additional studies, we performed microarray analysis and quantitative real-time PCR using heart tissues from *Braf*$^{Q241R/+}$; *Cre* embryos at E13.5 or E16.5. Interestingly, mRNA levels of dual specificity phosphatase (*Dusp*) 2, 4 and 6, that inactivate ERK, p38 or JNK, and *Spry* 1, which inhibits the RAS–MAPK signaling pathway, were significantly higher in *Braf*$^{Q241R/+}$; *Cre* embryos than those in *Braf*$^{+/+}$; *Cre* (data not shown). In the present study, constitutive activation of phosphorylated ERK was not clearly observed in whole embryos and heart tissues from *Braf*$^{Q241R/+}$; *Cre.* These results suggest that increased mRNA levels of *Dusp* 2, 4, 6 and *Spry* 1 and decreased expression of phosphorylated p38 in embryonic heart could represent a negative feedback mechanism for normalizing constitutive ERK activation in *Braf*$^{Q241R/+}$; *Cre* embryos.

In summary, *Braf* Q241R-expressing mice provided an effective tool for studying the pathogenesis of CFC syndrome. It was found for the first time that combination treatment with PD0325901 and GSK-J4 is efficacious for the treatment of mice with the activation of the RAS–MAPK pathway. At present, clinical trials of a new MEK inhibitor, MEK162, are now being conducted to investigate the efficacy and safety of its use in Noonan syndrome with hypertrophic cardiomyopathy as well as in individuals with solid tumors, while no clinical trial of histone H3K27 demethylase inhibitor has been performed. Given that *BRAF* mutations cause cancer, combination therapy with MEK inhibitors and histone H3K27 demethylase inhibitors can be effective not only for the treatment of patients with RASopathies but also for the treatment of *BRAF* mutation-associated cancer in the future.

MATERIALS AND METHODS

Generation of *Braf*^{Q241R} knockin mice

To construct the targeting vector for *Braf*^{Q241R} knockin mice, a short arm containing *Braf* exon 5 and 6 (*Not*I-*Sac*II genomic DNA fragment), a long arm including exon 7, 8 (*Xma*I–*Bam*HI genomic DNA fragment) and the downstream of exon 8 (*Bam*HI–*Sac*I) were amplified using a Roswell Park Cancer Institute-23 BAC clone. The DNA fragments were ligated into the pBSIISK+ vector. The *Braf* Q241R (exon 7) mutation was introduced by site-directed mutagenesis. The *Psp*0MI–*Xho*I site was used to insert PGK-Neo-STOP cassette flanked by loxP sites. The targeting vector was linearized with *Sal*I and electroporated into ES cells (C57BL/6J background). To confirm correctly targeted ES clones, we performed genotyping, sequencing and the test of the Cre-mediated recombination system. Furthermore, homologous recombinants were confirmed by Southern blotting using 5′, 3′ and Neo probes. For this experiment, genomic DNA was digested with *Sac*I (5′ probe), *Nco*I (3′ probe) or *Afl*II (Neo probe). The probe sequences are shown in Supplementary Material, Table S5. Screened ES clones were then microinjected into BALB/c blastocytes and the resulting chimeras were crossed with C57BL/6J mice to obtain *Braf*$^{Q241R\ Neo/+}$ heterozygotes mice. Excisions of the PGK-Neo cassette and STOP codon were achieved by crossing of *Braf*$^{Q241R\ Neo/+}$ heterozygotes with CAG-Cre transgenic mice (*Braf*$^{+/+}$; *Cre*) on C57BL/6J background (RIKEN BioResource Center, Tsukuba, Japan; RBRC01828) (49). Animal experiments were approved by the Animal Care and Use Committee of Tohoku University.

Genotyping

Genomic DNA was prepared from tail tissue with DNeasy Blood & Tissue Kit (Qiagen, Hilden, Germany) or Maxwell 16 Mouse Tail DNA Purification Kit (Promega, Madison, WI, USA). Genotyping of the *Braf*$^{+/+}$, *Braf*$^{+/+}$; *Cre*, *Braf*$^{Q241R\ Neo/+}$ and *Braf*$^{Q241R/+}$; *Cre* was carried out by PCR using KOD FX Neo (TOYOBO, Osaka, Japan) or TaKaRa Taq (Takara Bio, Otsu, Japan) with the primers shown in Supplementary Material, Table S6.

Sequencing

Total RNA was extracted with TRIzol reagent (Invitrogen, Carlsland, CA, USA), and cDNA was synthesized using High-Capacity cDNA Reverse Transcription Kit (Applied Biosystems, Foster City, CA, USA). The exonic region in *Braf* was amplified by PCR using TaKaRa Taq with the primers including M13 sequences: 5′-GTAAAACGACGGCCAGTGAAGTACT GGAGAATGTCCC-3′ and 5′-AGGAAACAGCTATGACCC CACATGTTTGACAACGGAAACCC-3′. The PCR products were purified with QIAquick Gel Extraction Kit (Qiagen, Tokyo, Japan) and sequenced on an ABI 3500xl automated DNA sequencer (Applied Biosystems).

Quantitative reverse transcription–PCR

Quantitative PCR was performed using FastStart Universal Probe Master (ROX) (Applied Biosystems) with StepOnePlus (Applied Biosystems). Amplification primers and hydrolysis probes were designed using Universal ProbeLibrary Assay Design Center (https://qpcr.probefinder.com/roche3.html).

Alcian Blue/Alizarin Red staining

After embryos were placed in water for a day, the skin and viscera were removed. The eviscerated embryos were then fixed in 95% ethanol for at least 3 days and stained with 150 mg/l Alcian Blue 8GX (Sigma-Aldrich, St. Louis, MO, USA), 80% ethanol and 20% acetic acid for 16–24 h. The stained embryos were rinsed with 95% ethanol and kept in 2% KOH for 16–24 h. They were then stained with 50 mg/l Alizarin Red (Sigma-Aldrich) and 1% KOH for 3 h, kept in 2% KOH for 12–48 h, placed in 20% glycerin/1% KOH for at least 5 days and stored in 50% glycerin.

Plasmid construction

The expression construct, including mouse *Braf* cDNA, was purchased from Origene (Rockville, MD, USA). PCR was performed using primers designed to introduce *Hin*dIII sites and the V5 epitope (C terminus). The PCR fragment was subcloned into pCR4-TOPO Vector (Invitrogen). The entire cDNA was verified by sequencing. The mutant constructs for *Braf* Q241R and V637E were generated using QuikChange Lightning Site-Directed Mutagenesis Kit (Stratagene, La Jolla, CA, USA) with the primers, 5′-CCGAAAGCTGCTTTTCCGGGGTTT CCGTTGTCAAA-3′ and 5′-TTTGACAACGGAAACCCCGG AAAAGCAGCTTTCGG-3′, and 5′-CTTTGGTCTAGCCACA GAGAAATCTCGGTGGAGTG-3′ and 5′-CACTCCACCGA GATTTCTCTGTGGCTAGACCAAAG-3′, respectively. All mutant constructs were verified by sequencing. The cDNAs were digested with *Hin*dIII, blunt-ended with T4 DNA polymerase and ligated into blunt-ended *Eco*RI site of pCAGGS vector (50).

Reporter assay

NIH 3T3 cells (ATCC, Rockville, MD, USA) were maintained in Dulbecco's modified Eagle's medium supplemented with 10% newborn calf serum, 50 U/ml penicillin and 50 μg/ml of streptomycin. The cells were seeded in 24-well plates at 3×10^5 cells/well 24 h before transfection. The cells were then transiently transfected using Lipofectamine and PLUS Reagent (Invitrogen) with 400 ng of pFR-luc, 25 ng of pFA2-Elk1, 5 ng of phRLnull-luc and 5 ng of WT or mutant expression constructs of *Braf*. Forty-eight hours after transfection, the cells were harvested in passive lysis buffer, and luciferase activity was assayed using Dual-Luciferase Reporter Assay System (Promega). Renilla luciferase expressed by phRLnull-luc was used to normalize the transfection efficiency.

Western blotting and phospho-kinase-antibody array

Whole-mouse embryos and brain were lysed in lysis buffer (10 mM Tris–HCl, pH 8.0 and 1% SDS), or genotype-confirmed hearts were pooled and lysed in the same buffer. These lysates were centrifuged at 14 000*g* for 15 min at 4°C and the protein concentration was determined by the Bradford method with Bio-Rad Protein Assay (Bio-Rad Laboratories, Hercules, CA, USA). Lysates were subjected to SDS–polyacrylamide gel electrophoresis (5–20% gradient gel; ATTO, Tokyo, Japan) and transferred to nitrocellulose membrane. Antibodies used were as follows (with catalog numbers in parentheses): B-RAF (9434), ERK1/2 (9102), phospho-ERK1/2 (9101), phospho-MEK (9121), p38 (9212), phospho-p38 (4511), phospho-SAPK/JNK (4668), AKT (9272), phospho-AKT (on Ser473; 9018) and phospho-AKT (on Thr308; 2965) from Cell Signaling (Danvers, MA, USA). C-RAF (610152), MEK (sc-219) and β-actin (A5316) were from BD Transduction Laboratories (San Jose, CA, USA), Santa Cruz Biotechnology (Santa Cruz, CA, USA) and Sigma-Aldrich, respectively. All the membranes were visualized using Western Lightning ECL-Plus Kit (Perkin-Elmer, Waltham, MA, USA). The band intensities were quantified using ImageJ software (http://rsbweb.nih.gov/ij/) and normalized to β-actin. Phosphorylated protein was measured to determine the ratios of phosphorylated protein to non-phosphorylated protein and then normalized to β-actin.

For kinase-antibody arrays, protein extracts of embryonic hearts (400 μg) were incubated with the Phospho-Kinase Antibody Array Kit (Proteome Profiler Antibody Array; R&D systems, Minneapolis, MN, USA) following the manufacturer's instructions.

Histology and immunohistochemistry

Embryonic hearts were perfused with phosphate-buffered saline and 10% neutral buffered formalin from the placenta. The fixed hearts and whole-mouse embryos fixed in 10% neutral buffered formalin were embedded in paraffin. Embedded tissues were sectioned at 6 μm (hearts) or 3 μm (whole-mouse embryos and lungs). Sections were stained with hematoxylin and eosin. In hearts from embryos at E16.5, the largest diameters of the ventricular radius were measured in serial coronal sections where a four-chamber view was observed. The largest thicknesses of cardiac valve leaflets in serial sections were measured. Edematous and dead embryos were excluded from these analyses.

For immunohistochemistry, the antibodies used were as follows (with catalog numbers in parentheses): phospho-Histone H3 (9701) from Cell Signaling, LYVE-1 (103-PA50AG) from RELIA Tech GmbH (Braunschweig, Germany), α-SMA (M0851) from DAKO (Glostrup, Denmark), PECAM-1 (CD31; sc-1506) from Santa Cruz Biotechnology and TTF-1 (MS-669-P1ABX) from Thermo Fisher Scientific (Fremont, CA, USA). Signals were amplified by Histofine Simple Stain (Nichirei Bio Sciences, Tokyo, Japan) and color was developed by DAB Substrate Kit (Nichirei Bio Sciences). Sections were counterstained with hematoxylin.

PAS staining

Deparaffinized lung sections were incubated in 0.5% periodic acid for 10 min at 60°C, rinsed with distilled water and stained in Schiff's reagent (Muto Pure Chemicals, Tokyo, Japan) for 10 min. Stained slides were counterstained with hematoxylin, dehydrated and mounted.

Animal treatment

Stock solution of PD0325901 (Sigma-Aldrich) was prepared using ethanol, whereas those of MAZ-51 (Calbiochem, San Diego, CA, USA), Sorafenib (Toronto Research Chemicals, North York, ON, USA), Lovastatin (Calbiochem), Everolimus (Selleckchem, Houston, TX, USA), NCDM-32b (Wako Pure Chemicals, Osaka, Japan), GSK-J4 (Cayman Chemical) and the combination of PD0325901 and GSK-J4 were prepared using dimethylsulfoxide. PD0325901 was resuspended in saline while and all other reagents were resuspended in 0.5% hydroxypropylmethylcellulose with 0.2% Tween80, respectively. The prepared reagents or vehicles were i.p. injected into pregnant mice daily, beginning on E10.5 and continuing till E15.5 or E18.5.

Statistical analysis

All statistical analysis was performed using Prism software (ver. 6.01; GraphPad Software, Inc., San Diego, CA, USA). Data analysis were performed with Student's *t*-test for unpaired samples, one-way analysis of variance followed by the Tukey–Kramer test for comparison of multiple experimental groups and the χ^2 test for differences between observed and expected distributions. Differences were considered significant at a *P*-value of < 0.05.

SUPPLEMENTARY MATERIAL

Supplementary Material is available at *HMG* online.

ACKNOWLEDGEMENTS

We are grateful to Jun-ichi Miyazaki, Osaka University, for supplying the pCAGGS expression vector. We thank Riyo Takahashi, Kumi Kato, Yoko Tateda and Daisuke Akita for technical assistance and Fumiko Date for technical assistance and for discussion of the experimental data. We also acknowledge the support of the Biomedical Research Core of Tohoku University Graduate School of Medicine. We thank RIKEN BioResource Center for providing us with B6.Cg-Tg(CAG-Cre)CZ-MO2Osb mice (RBRC01828).

Conflict of Interest statement. None declared.

FUNDING

This work was supported by the Funding Program for the Next Generation of World-Leading Researchers (NEXT Program) from the Ministry of Education, Culture, Sports, Science and Technology of Japan to Y.A. (LS004), by Grants-in-Aids from the Ministry of Education, Culture, Sports, Science and Technology of Japan, the Ministry of Health, Labor and Welfare, and the Japan Society for the Promotion of Science (JSPS) KAKENHI Grant number 26293241 to Y.A., and by JSPS KAKENHI Grant number 25860839 to S.I.

REFERENCES

1. Reynolds, J.F., Neri, G., Herrmann, J.P., Blumberg, B., Coldwell, J.G., Miles, P.V. and Opitz, J.M. (1986) New multiple congenital anomalies/mental retardation syndrome with cardio-facio-cutaneous involvement – the CFC syndrome. *Am. J. Med. Genet.*, **25**, 413–427.
2. Witters, I., Denayer, E., Brems, H., Fryns, J.P. and Legius, E. (2008) The cardiofaciocutaneous syndrome: prenatal findings in two patients. *Prenat. Diagn.*, **28**, 53–55.
3. Niihori, T., Aoki, Y., Narumi, Y., Neri, G., Cave, H., Verloes, A., Okamoto, N., Hennekam, R.C., Gillessen-Kaesbach, G., Wieczorek, D. *et al.* (2006) Germline KRAS and BRAF mutations in cardio-facio-cutaneous syndrome. *Nat. Genet.*, **38**, 294–296.
4. Rodriguez-Viciana, P., Tetsu, O., Tidyman, W.E., Estep, A.L., Conger, B.A., Cruz, M.S., McCormick, F. and Rauen, K.A. (2006) Germline mutations in genes within the MAPK pathway cause cardio-facio-cutaneous syndrome. *Science*, **311**, 1287–1290.
5. Narumi, Y., Aoki, Y., Niihori, T., Neri, G., Cave, H., Verloes, A., Nava, C., Kavamura, M.I., Okamoto, N., Kurosawa, K. *et al.* (2007) Molecular and clinical characterization of cardio-facio-cutaneous (CFC) syndrome: overlapping clinical manifestations with Costello syndrome. *Am. J. Med. Genet. A*, **143A**, 799–807.
6. Abe, Y., Aoki, Y., Kuriyama, S., Kawame, H., Okamoto, N., Kurosawa, K., Ohashi, H., Mizuno, S., Ogata, T., Kure, S. *et al.* (2012) Prevalence and clinical features of Costello syndrome and cardio-facio-cutaneous syndrome in Japan: findings from a nationwide epidemiological survey. *Am. J. Med. Genet. A*, **158A**, 1083–1094.
7. Malumbres, M. and Barbacid, M. (2003) RAS oncogenes: the first 30 years. *Nat. Rev. Cancer*, **3**, 459–465.
8. Aoki, Y., Niihori, T., Banjo, T., Okamoto, N., Mizuno, S., Kurosawa, K., Ogata, T., Takada, F., Yano, M., Ando, T. *et al.* (2013) Gain-of-function mutations in RIT1 cause Noonan syndrome, a RAS/MAPK pathway syndrome. *Am. J. Hum. Genet.*, **93**, 173–180.
9. Aoki, Y., Niihori, T., Narumi, Y., Kure, S. and Matsubara, Y. (2008) The RAS/MAPK syndromes: novel roles of the RAS pathway in human genetic disorders. *Hum. Mutat.*, **29**, 992–1006.
10. Tidyman, W.E. and Rauen, K.A. (2009) The RASopathies: developmental syndromes of Ras/MAPK pathway dysregulation. *Curr. Opin. Genet. Dev.*, **19**, 230–236.
11. Davies, H., Bignell, G.R., Cox, C., Stephens, P., Edkins, S., Clegg, S., Teague, J., Woffendin, H., Garnett, M.J., Bottomley, W. *et al.* (2002) Mutations of the BRAF gene in human cancer. *Nature*, **417**, 949–954.
12. Andreadi, C., Cheung, L.K., Giblett, S., Patel, B., Jin, H., Mercer, K., Kamata, T., Lee, P., Williams, A., McMahon, M. *et al.* (2012) The intermediate-activity (L597 V) BRAF mutant acts as an epistatic modifier of oncogenic RAS by enhancing signaling through the RAF/MEK/ERK pathway. *Genes Dev.*, **26**, 1945–1958.
13. Sarkozy, A., Carta, C., Moretti, S., Zampino, G., Digilio, M.C., Pantaleoni, F., Scioletti, A.P., Esposito, G., Cordeddu, V., Lepri, F. *et al.* (2009) Germline BRAF mutations in Noonan, LEOPARD, and cardiofaciocutaneous syndromes: molecular diversity and associated phenotypic spectrum. *Hum. Mutat.*, **30**, 695–702.
14. Storm, S.M., Cleveland, J.L. and Rapp, U.R. (1990) Expression of raf family proto-oncogenes in normal mouse tissues. *Oncogene*, **5**, 345–351.
15. Wojnowski, L., Stancato, L.F., Larner, A.C., Rapp, U.R. and Zimmer, A. (2000) Overlapping and specific functions of Braf and Craf-1 proto-oncogenes during mouse embryogenesis. *Mech. Dev.*, **91**, 97–104.
16. Wojnowski, L., Zimmer, A.M., Beck, T.W., Hahn, H., Bernal, R., Rapp, U.R. and Zimmer, A. (1997) Endothelial apoptosis in Braf-deficient mice. *Nat. Genet.*, **16**, 293–297.
17. Mercer, K., Giblett, S., Green, S., Lloyd, D., DaRocha Dias, S., Plumb, M., Marais, R. and Pritchard, C. (2005) Expression of endogenous oncogenic V600E B-raf induces proliferation and developmental defects in mice and transformation of primary fibroblasts. *Cancer Res.*, **65**, 11493–11500.
18. Urosevic, J., Sauzeau, V., Soto-Montenegro, M.L., Reig, S., Desco, M., Wright, E.M., Canamero, M., Mulero, F., Ortega, S., Bustelo, X.R. *et al.* (2011) Constitutive activation of B-Raf in the mouse germ line provides a model for human cardio-facio-cutaneous syndrome. *Proc. Natl. Acad. Sci. USA*, **108**, 5015–5020.
19. Watanabe, Y., Miyagawa-Tomita, S., Vincent, S.D., Kelly, R.G., Moon, A.M. and Buckingham, M.E. (2010) Role of mesodermal FGF8 and FGF10 overlaps in the development of the arterial pole of the heart and pharyngeal arch arteries. *Circ. Res.*, **106**, 495–503.
20. Packer, L.M., East, P., Reis-Filho, J.S. and Marais, R. (2009) Identification of direct transcriptional targets of (V600E)BRAF/MEK signalling in melanoma. *Pigment Cell Melanoma Res.*, **22**, 785–798.
21. Deng, Y., Atri, D., Eichmann, A. and Simons, M. (2013) Endothelial ERK signaling controls lymphatic fate specification. *J. Clin. Invest.*, **123**, 1202–1215.
22. Bekker, M.N., Twisk, J.W., Bartelings, M.M., Gittenberger-de Groot, A.C. and van Vugt, J.M. (2006) Temporal relationship between increased nuchal translucency and enlarged jugular lymphatic sac. *Obstet. Gynecol.*, **108**, 846–853.
23. Makinen, T., Norrmen, C. and Petrova, T.V. (2007) Molecular mechanisms of lymphatic vascular development. *Cell Mol. Life Sci.*, **64**, 1915–1929.
24. Chen, P.C., Wakimoto, H., Conner, D., Araki, T., Yuan, T., Roberts, A., Seidman, C., Bronson, R., Neel, B., Seidman, J.G. *et al.* (2010) Activation of multiple signaling pathways causes developmental defects in mice with a Noonan syndrome-associated Sos1 mutation. *J. Clin. Invest.*, **120**, 4353–4365.
25. Kruidenier, L., Chung, C.W., Cheng, Z., Liddle, J., Che, K., Joberty, G., Bantscheff, M., Bountra, C., Bridges, A., Diallo, H. *et al.* (2012) A selective jumonji H3K27 demethylase inhibitor modulates the proinflammatory macrophage response. *Nature*, **488**, 404–408.

26. Lee, S., Lee, J.W. and Lee, S.K. (2012) UTX, a histone H3-lysine 27 demethylase, acts as a critical switch to activate the cardiac developmental program. *Dev. Cell*, **22**, 25–37.
27. Welstead, G.G., Creyghton, M.P., Bilodeau, S., Cheng, A.W., Markoulaki, S., Young, R.A. and Jaenisch, R. (2012) X-linked H3K27me3 demethylase Utx is required for embryonic development in a sex-specific manner. *Proc. Natl. Acad. Sci. USA*, **109**, 13004–13009.
28. Zaidi, S., Choi, M., Wakimoto, H., Ma, L., Jiang, J., Overton, J.D., Romano-Adesman, A., Bjornson, R.D., Breitbart, R.E., Brown, K.K. *et al.* (2013) De novo mutations in histone-modifying genes in congenital heart disease. *Nature*, **498**, 220–223.
29. Hamada, S., Suzuki, T., Mino, K., Koseki, K., Oehme, F., Flamme, I., Ozasa, H., Itoh, Y., Ogasawara, D., Komaarashi, H. *et al.* (2010) Design, synthesis, enzyme-inhibitory activity, and effect on human cancer cells of a novel series of jumonji domain-containing protein 2 histone demethylase inhibitors. *J. Med. Chem.*, **53**, 5629–5638.
30. Croonen, E.A., Nillesen, W.M., Stuurman, K.E., Oudesluijs, G., van de Laar, I.M., Martens, L., Ockeloen, C., Mathijssen, I.B., Schepens, M., Ruiterkamp-Versteeg, M. *et al.* (2013) Prenatal diagnostic testing of the Noonan syndrome genes in fetuses with abnormal ultrasound findings. *Eur. J. Hum. Genet.*, **21**, 936–942.
31. Nisbet, D.L., Griffin, D.R. and Chitty, L.S. (1999) Prenatal features of Noonan syndrome. *Prenat. Diagn.*, **19**, 642–647.
32. de Mooij, Y.M., van den Akker, N.M., Bekker, M.N., Bartelings, M.M., van Vugt, J.M. and Gittenberger-de Groot, A.C. (2011) Aberrant lymphatic development in euploid fetuses with increased nuchal translucency including Noonan syndrome. *Prenat. Diagn.*, **31**, 159–166.
33. Romano, A.A., Allanson, J.E., Dahlgren, J., Gelb, B.D., Hall, B., Pierpont, M.E., Roberts, A.E., Robinson, W., Takemoto, C.M. and Noonan, J.A. (2010) Noonan syndrome: clinical features, diagnosis, and management guidelines. *Pediatrics*, **126**, 746–759.
34. Marin, T.M., Keith, K., Davies, B., Conner, D.A., Guha, P., Kalaitzidis, D., Wu, X., Lauriol, J., Wang, B., Bauer, M. *et al.* (2011) Rapamycin reverses hypertrophic cardiomyopathy in a mouse model of LEOPARD syndrome-associated PTPN11 mutation. *J. Clin. Invest.*, **121**, 1026–1043.
35. Wu, X., Simpson, J., Hong, J.H., Kim, K.H., Thavarajah, N.K., Backx, P.H., Neel, B.G. and Araki, T. (2011) MEK-ERK pathway modulation ameliorates disease phenotypes in a mouse model of Noonan syndrome associated with the Raf1(L613 V) mutation. *J. Clin. Invest.*, **121**, 1009–1025.
36. Schuhmacher, A.J., Guerra, C., Sauzeau, V., Canamero, M., Bustelo, X.R. and Barbacid, M. (2008) A mouse model for Costello syndrome reveals an Ang II-mediated hypertensive condition. *J. Clin. Invest.*, **118**, 2169–2179.
37. Kooistra, S.M. and Helin, K. (2012) Molecular mechanisms and potential functions of histone demethylases. *Nat. Rev. Mol. Cell. Biol.*, **13**, 297–311.
38. He, A., Ma, Q., Cao, J., von Gise, A., Zhou, P., Xie, H., Zhang, B., Hsing, M., Christodoulou, D.C., Cahan, P. *et al.* (2012) Polycomb repressive complex 2 regulates normal development of the mouse heart. *Circ. Res.*, **110**, 406–415.
39. Lederer, D., Grisart, B., Digilio, M.C., Benoit, V., Crespin, M., Ghariani, S.C., Maystadt, I., Dallapiccola, B. and Verellen-Dumoulin, C. (2012) Deletion of KDM6A, a histone demethylase interacting with MLL2, in three patients with Kabuki syndrome. *Am. J. Hum. Genet.*, **90**, 119–124.
40. Inagawa, M., Nakajima, K., Makino, T., Ogawa, S., Kojima, M., Ito, S., Ikenishi, A., Hayashi, T., Schwartz, R.J., Nakamura, K. *et al.* (2013) Histone H3 lysine 9 methyltransferases, G9a and GLP are essential for cardiac morphogenesis. *Mech. Dev.*, **130**, 519–531.
41. Kretzschmar, M., Doody, J., Timokhina, I. and Massague, J. (1999) A mechanism of repression of TGFbeta/ Smad signaling by oncogenic Ras. *Genes Dev.*, **13**, 804–816.
42. Agger, K., Cloos, P.A., Rudkjaer, L., Williams, K., Andersen, G., Christensen, J. and Helin, K. (2009) The H3K27me3 demethylase JMJD3 contributes to the activation of the INK4A-ARF locus in response to oncogene- and stress-induced senescence. *Genes Dev.*, **23**, 1171–1176.
43. Fujii, S., Tokita, K., Wada, N., Ito, K., Yamauchi, C., Ito, Y. and Ochiai, A. (2011) MEK-ERK pathway regulates EZH2 overexpression in association with aggressive breast cancer subtypes. *Oncogene*, **30**, 4118–4128.
44. Krenz, M., Gulick, J., Osinska, H.E., Colbert, M.C., Molkentin, J.D. and Robbins, J. (2008) Role of ERK1/2 signaling in congenital valve malformations in Noonan syndrome. *Proc. Natl. Acad. Sci. USA*, **105**, 18930–18935.
45. Wan, P.T., Garnett, M.J., Roe, S.M., Lee, S., Niculescu-Duvaz, D., Good, V.M., Jones, C.M., Marshall, C.J., Springer, C.J., Barford, D. *et al.* (2004) Mechanism of activation of the RAF-ERK signaling pathway by oncogenic mutations of B-RAF. *Cell*, **116**, 855–867.
46. Pierpont, E.I., Pierpont, M.E., Mendelsohn, N.J., Roberts, A.E., Tworog-Dube, E., Rauen, K.A. and Seidenberg, M.S. (2010) Effects of germline mutations in the Ras/MAPK signaling pathway on adaptive behavior: cardiofaciocutaneous syndrome and Noonan syndrome. *Am. J. Med. Genet. A*, **152A**, 591–600.
47. Stevenson, D.A., Schwarz, E.L., Carey, J.C., Viskochil, D.H., Hanson, H., Bauer, S., Weng, H.Y., Greene, T., Reinker, K., Swensen, J. *et al.* (2011) Bone resorption in syndromes of the Ras/MAPK pathway. *Clin. Genet.*, **80**, 566–573.
48. Armour, C.M. and Allanson, J.E. (2008) Further delineation of cardio-facio-cutaneous syndrome: clinical features of 38 individuals with proven mutations. *J. Med. Genet.*, **45**, 249–254.
49. Matsumura, H., Hasuwa, H., Inoue, N., Ikawa, M. and Okabe, M. (2004) Lineage-specific cell disruption in living mice by Cre-mediated expression of diphtheria toxin A chain. *Biochem. Biophys. Res. Commun.*, **321**, 275–279.
50. Niwa, H., Yamamura, K. and Miyazaki, J. (1991) Efficient selection for high-expression transfectants with a novel eukaryotic vector. *Gene*, **108**, 193–199.

Available online at www.sciencedirect.com

ScienceDirect

Neuromuscular Disorders 24 (2014) 1068–1072

www.elsevier.com/locate/nmd

Case report

GNE myopathy associated with congenital thrombocytopenia: A report of two siblings

Rumiko Izumi [a,b], Tetsuya Niihori [a], Naoki Suzuki [b], Yoji Sasahara [c], Takeshi Rikiishi [c], Ayumi Nishiyama [a,b], Shuhei Nishiyama [b], Kaoru Endo [b], Masaaki Kato [b], Hitoshi Warita [b], Hidehiko Konno [d], Toshiaki Takahashi [d], Maki Tateyama [b], Takeshi Nagashima [e], Ryo Funayama [e], Keiko Nakayama [e], Shigeo Kure [c], Yoichi Matsubara [a], Yoko Aoki [a], Masashi Aoki [b,*]

[a] *Department of Medical Genetics, Tohoku University School of Medicine, Sendai, Japan*
[b] *Department of Neurology, Tohoku University School of Medicine, Sendai, Japan*
[c] *Department of Pediatrics, Tohoku University School of Medicine, Sendai, Japan*
[d] *Department of Neurology and Division of Clinical Research, Sendai Nishitaga National Hospital, Sendai, Japan*
[e] *Division of Cell Proliferation, United Centers for Advanced Research and Translational Medicine, Tohoku University Graduate School of Medicine, Sendai, Japan*

Received 2 May 2014; received in revised form 13 July 2014; accepted 30 July 2014

Abstract

GNE myopathy is an autosomal recessive muscular disorder caused by mutations in the gene encoding the key enzyme in sialic acid biosynthesis, UDP-N-acetylglucosamine 2-epimerase/N-acetylmannosamine kinase (GNE/MNK). Here, we report two siblings with myopathy with rimmed vacuoles and congenital thrombocytopenia who harbored two compound heterozygous *GNE* mutations, p.V603L and p.G739S. Thrombocytopenia, which is characterized by shortened platelet lifetime rather than ineffective thrombopoiesis, has been observed since infancy. We performed exome sequencing and array CGH to identify the underlying genetic etiology of thrombocytopenia. No pathogenic variants were detected among the known causative genes of recessively inherited thrombocytopenia; yet, candidate variants in two genes that followed an autosomal recessive mode of inheritance, including previously identified *GNE* mutations, were detected. Alternatively, it is possible that the decreased activity of GNE/MNK itself, which would lead to decreased sialic content in platelets, is associated with thrombocytopenia in these patients. Further investigations are required to clarify the association between *GNE* myopathy and the pathogenesis of thrombocytopenia.

Keywords: *GNE*; Distal myopathy with rimmed vacuoles; Sialic acid; UDP-N-acetylglucosamine 2-epimerase/N-acetylmannosamine kinase; Thrombocytopenia; Exome sequencing

1. Introduction

GNE myopathy is a group of autosomal recessive muscular disorders caused by mutations in *GNE*, which encodes the key enzyme of sialic acid biosynthesis, UDP-N-acetylglucosamine 2-epimerase/N-acetylmannosamine kinase (GNE/MNK). This enzyme initiates and regulates the biosynthesis of

* Corresponding author. Address: Department of Neurology, Tohoku University School of Medicine, 1-1 Seiryo-machi, Aoba-ku, Sendai 980-8574, Japan. Tel.: +81 22 717 7189; fax: +81 22 717 7192.
E-mail address: aokim@med.tohoku.ac.jp (M. Aoki).

http://dx.doi.org/10.1016/j.nmd.2014.07.008
0960-8966/

N-acetylneuraminic acid [1], a substrate for sialylation. *GNE* mutations have been identified in both hereditary inclusion body myopathy [2,3] and Nonaka myopathy, which is also called distal myopathy with rimmed vacuoles (DMRV; MIM#605820) [4,5]. Since these conditions have been confirmed to be the same, they are now generically referred to as *GNE* myopathy.

Here, we report two siblings with compound heterozygous *GNE* mutations who manifested a myopathy with rimmed vacuoles associated with thrombocytopenia. The phenotypes of patients with *GNE* myopathy are variable; however, hematological complications are rare. To identify the underlying genetic etiology of thrombocytopenia in these siblings, we performed exome sequencing and array CGH. The possibility of a genetic defect in sialic acid biosynthesis as a cause of thrombocytopenia is also discussed.

2. Case report

2.1. Patients

The siblings described in this study are of Japanese ancestry and the only offspring of nonconsanguineous parents. Their parents and other family members have no medical history of hematological or neuromuscular disorders.

Patient 1 is a 32-year-old man and the thrombocytopenia was detected during treatment for neonatal jaundice. His thrombocytopenia persisted, with a platelet count ranging from 1.7×10^9/L to 16.2×10^9/L. He had no other congenital abnormalities or developmental delays. Megakaryocytes in the bone marrow, observed at the age of 8 years, were morphologically normal and increased in number to 281/mm^3, and his nuclear cell count was normal at 37.4×10^4/mm^3. The size of his peripheral blood platelets was normal to large, and the mean platelet volume was 10–11 fl. Platelet-associated IgG (PAIgG) was elevated (207.3 ng/10^7 cells), and von Willebrand factor activity was within the normal range. At the age of 7 years, proteinuria and hematuria were detected. Kidney biopsy revealed atypical membranoproliferative glomerulonephritis, which later progressed to chronic renal failure requiring periodic dialysis therapy. He had a waddling gait that began in middle adolescence and muscle weakness that gradually progressed, particularly in the proximal lower limbs. Neurological examination at the age of 20 years showed proximal muscle weakness, particularly in the neck flexor and iliopsoas. His serum creatine kinase levels ranged from 300 to 600 IU/L. Muscle biopsy specimens taken from the rectus femoris of Pathological findings of the rectus femoris showed increased rimmed vacuoles in approximately 1% of myofibers, located predominantly in atrophic fibers. Necrotic and regenerating fibers were rare, and no inflammatory cellular infiltration was observed. Mutation analysis of *GNE* identified the following two missense mutations: c.1807G > C (NM_001128227); p.V603L (NP_001121699) and c.2215G > A; p.G739S, both of which have been reported previously as causes of DMRV [6,7]. Parental analysis confirmed that he was a compound heterozygote for these mutations. He has been wheelchair-bound since the age of 24 years. From the age of 22 years, he has had mildly decreased cardiac function accompanied by mitral insufficiency, but his respiratory system has remained fully functional so far.

Patient 2, a 29-year-old woman, is the younger sister of Patient 1. Her thrombocytopenia was incidentally found at the age of 2 years while undergoing treatment for pneumonia. Her thrombocytopenia persisted, with a platelet count ranging from 1.1×10^9/L to 9.0×10^9/L. This induced intermittent nasal bleeding. Megakaryocytes in her bone marrow, observed at the age of 5 years, were normal in number and morphology. Her platelets were normal to large in size, with a mean volume of 10–13 fl (Fig. 1), and her PAIgG was elevated (119 ng/10^7 cells). At the age of 18 years, she exhibited proximal muscle weakness accompanied by difficulties in standing and lifting her arms. At the age of 23 years, her muscle strength decreased in the neck and overall proximal muscles, and she developed a waddling gait. Muscle imaging showed remarkable atrophy in the paraspinal muscles and moderate patchy atrophy in the adductor magnus, soleus and tibialis posterior muscles. Her serum creatine kinase level was elevated (360 IU/L). Pathological findings of the biceps brachii were essentially similar to those of Patient 1 (Fig. 2). Genetic testing for *GNE* indicated that she also harbored the p.V603L and p.G739S mutations. Systemic examination revealed moderate splenomegaly, but normal cardiorespiratory and renal functions were maintained. She is still able to walk independently with a simple walking aid.

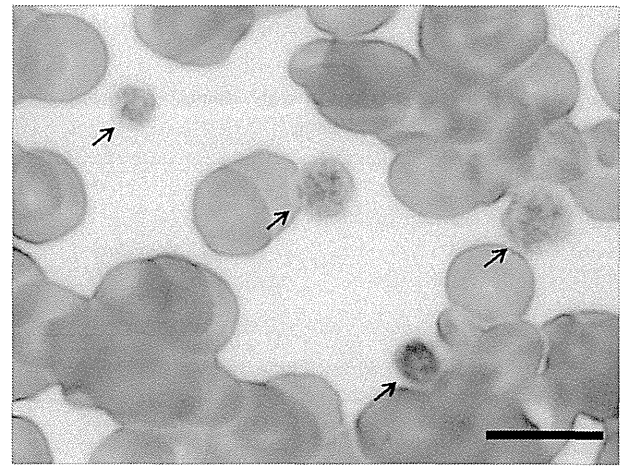

Fig. 1. Morphology of peripheral blood platelets a blood smear from Patient 2 showing morphologically normal platelets (arrow). The size of platelets was normal to large. Bars = 10 μm.

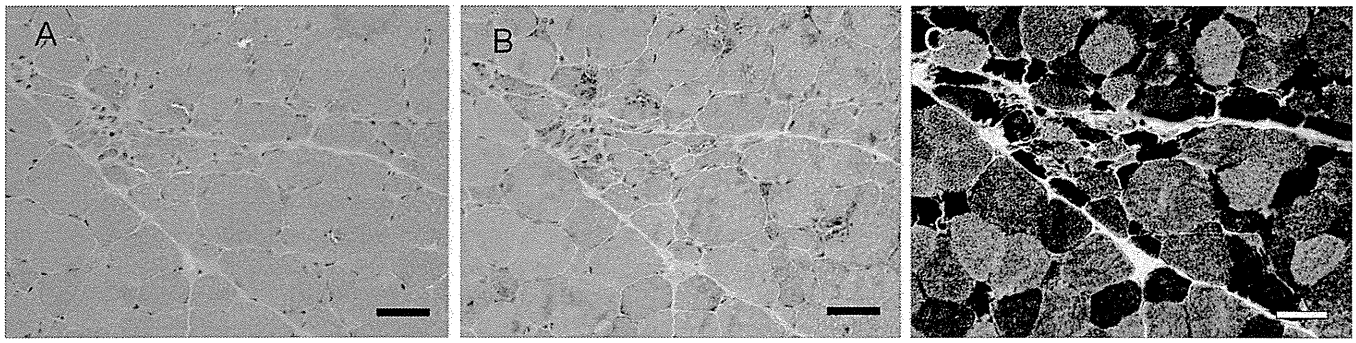

Fig. 2. Pathology of the muscle biopsy specimens hematoxylin-eosin (A), Gomori-trichrome (B) and NADH-tetrazolium reductase (C) staining of the muscle biopsy sample from the biceps brachii of patient 2 are shown. Atrophic fibers were clustering into small groups, including both type 1 and type 2 myofibers. Several rimmed vacuoles were scattered around them predominantly located on atrophic fibers. NADH-tetrazolium reductase staining showed an almost normal myofibrillar network. Bars = 50 μm.

2.2. Exome sequencing and array CGH

Exome sequencing and array CGH were performed on peripheral blood samples from the siblings and their parents to determine the genetic cause of thrombocytopenia. This study was approved by the Ethics Committee of the Tohoku University School of Medicine, and all individuals gave their informed consent prior to their inclusion in the study.

2.2.1. Exome sequencing

The detailed methods regarding exome sequencing were described in our previous report [8]. After excluding synonymous SNVs, we used the 1000 Genomes to filter out frequent variants. Three pairs of rare variants (i.e., not present or <1% allele frequency according to the 1000 Genomes), which were segregated in an autosomal recessive mode, were identified in *CPEB2, FLNB* and *GNE* (Supplementary Tables 1 and 2). The mutation in *CPEB2* was present with 13.7% allele frequency and with 1.9% in homozygous state according to Human Genetic Variation Database (http://www.genome.med.kyoto-u.ac.jp/SnpDB/), thus seemed less pathogenic. Exome sequencing enabled comprehensive screening for the causative genes of recessively inherited thrombocytopenia with coverage of 95% of all targeted regions at ⩾20-fold and we did not detect any novel or rare homozygous or compound heterozygous mutations among these genes (Supplementary Table 3).

2.2.2. Array CGH

Array CGH was performed using the Agilent SurePrint G3 Human Custom CNV 2 × 400 K microarray for all individuals, and it revealed three regions with recessively inherited deletions of genomic copy number (Supplementary Table 4). None of the genes in or around these deleted regions have been previously reported as being responsible for myopathy or thrombocytopenia.

3. Discussion

In this study, we described two siblings harboring two compound heterozygous *GNE* mutations, p.V603L and p.G739S, who were diagnosed with myopathy with rimmed vacuoles associated with congenital thrombocytopenia.

The pathogenesis of thrombocytopenia involves various congenital or acquired disorders. Familial occurrence of thrombocytopenia in the neonatal period and infancy strongly suggests the involvement of a genetic defect. Hereditary thrombocytopenia is extremely heterogeneous in terms of the gene mutations involved, although the genetic background contributing to this condition remains to be elucidated [9]. Exome sequencing identified substantially two pairs of rare compound heterozygous variants in *FLNB* and *GNE*, which cosegregated in a recessive mode (Supplementary Table 2). The one encoding filamin b is highly homologous to the gene encoding filamin a (*FLNA*), which is located on chromosome Xq28. Although a missense mutation in *FLNA* has been reported as a cause of nonsyndromic thrombocytopenia [10], the pathogenicity of *FLNB* variants in this family remains unknown.

GNE mutations result in the loss of its enzymatic activity and failure to catalyze the initial two steps in sialic acid biosynthesis, leading to decreased sialic acid content in the organs [11]. This hyposialylation and abnormal glycosylation in muscles have been thought to contribute to the pathogenesis of *GNE* myopathy [12]. In this context, hyposialylation caused by *GNE* mutations may be a common defect in muscles and platelets. Sialic acid is known to play significant roles in platelet function, is located in the platelet membrane, and forms a part of glycosylation. Several groups have shown that platelets deficient in sialylation are easily removed from circulation, resulting in shortened circulation lifetimes and thrombocytopenia [13–15]. Decreased sialic acid content in platelets has also been reported in

infection-induced thrombosis [16], and hepatic cirrhosis [17]. These findings suggest that sialic acid is an essential molecule for the stabilization of circulating platelets, and hyposialylation of platelets can be a general risk factor for thrombocytopenia.

Recently, another group reported a family with distal myopathy with rimmed vacuoles associated with thrombocytopenia [18]; they suggested that two novel specific *GNE* mutations identified in the affected siblings, p.Y217H and p.D515Qfs*2, may have led to thrombocytopenia. In contrast, the p.V603L mutation identified in our cases is the most common among the Japanese population [5,6], while the p.G739S mutation occurs rather infrequently [7,19,20]. However, it still remains unknown whether thrombocytopenia is associated with *GNE* myopathy in general or rather with these specific *GNE* mutations. Careful observation of the hematologic features in other patients with *GNE* myopathy will reveal whether *GNE* myopathy is frequently associated with thrombocytopenia.

The reason for elevated PAIgG observed in our cases remains unknown. PAIgG is elevated in patients with immune and nonimmune thrombocytopenia, and its pathogenic effect has not been fully established [21]. Dysregulation of immune system has not been reported in individuals with *GNE* myopathy. However, a past report showed that the removal of sialic acid from platelet membranes and an increase in PAIgG were observed in baboons, suggesting that the loss of sialic acid may have exposed senescent cell antigens [14]. Further analysis will be necessary to clarify the mechanism of elevated PAIgG in our cases.

Patient 1 manifested atypical membranoproliferative glomerulonephritis with proteinuria and hematuria. The renal pathology including diffuse thickening of the glomerular basement membrane with the appearance of double contours is similar to those reported in *GNE* mutant mice [22,23], suggesting his nephritic phenotype is associated with *GNE* mutations. Membranoproliferative glomerulonephritis is sometimes accompanied by thrombocytopenia from platelet consumption. However the early onset of thrombocytopenia and patient 2's maintained renal function mean the mechanism of their thrombocytopenia is independent of renal pathology.

In conclusion, we described two siblings with the *GNE* mutations, p.V603L and p.G739S, who manifested both myopathy and thrombocytopenia. Genetic alterations to known causative genes for autosomal recessive thrombocytopenia were not identified by exome sequencing. Therefore, we could not conclude whether the rare candidate variants detected by exome sequencing or the deletions identified by array CGH had any pathogenic role in thrombocytopenia observed in our cases. Hence, further investigations are required to clarify the possible association between *GNE* myopathy and the pathogenesis of thrombocytopenia observed in these patients.

Acknowledgments

We thank the patients and their parents. We are also grateful to Drs. Shigeru Tsuchiya and Madoka Mori for their fruitful discussion and Yoko Tateda, Kumi Kato, Naoko Shimakura, Risa Ando, Riyo Takahashi, Miyuki Tsuda, Makiko Nakagawa, Mami Kikuchi, and Kiyotaka Kuroda for their technical assistance. We also acknowledge the support of the Biomedical Research Core of Tohoku University Graduate School of Medicine. This work was supported by a grant for Research on Applying Health Technology provided by the Ministry of Health, Labor and Welfare to YM and an Intramural Research Grant (23-5) for Neurological and Psychiatric Disorders of NCNP, JSPS KAKENHI (Grant Number 24659421) and Research on Measures for Intractable Diseases from the Japanese Ministry of Health, Labor and Welfare to MA.

Appendix A. Supplementary data

Supplementary data associated with this article can be found, in the online version, at http://dx.doi.org/10.1016/j.nmd.2014.07.008.

References

[1] Stasche R, Hinderlich S, Weise C, et al. A bifunctional enzyme catalyzes the first two steps in N-acetylneuraminic acid biosynthesis of rat liver. Molecular cloning and functional expression of UDP-N-acetyl-glucosamine 2-epimerase/N-acetylmannosamine kinase. J Biol Chem 1997;272:24319–24.

[2] Argov Z, Yarom R. "Rimmed vacuole myopathy" sparing the quadriceps. A unique disorder in Iranian Jews. J Neurol Sci 1984;64:33–43.

[3] Eisenberg I, Avidan N, Potikha T, et al. The UDP-N-acetylglucosamine 2-epimerase/N-acetylmannosamine kinase gene is mutated in recessive hereditary inclusion body myopathy. Nat Genet 2001;29:83–7.

[4] Nonaka I, Sunohara N, Ishiura S, Satoyoshi E. Familial distal myopathy with rimmed vacuole and lamellar (myeloid) body formation. J Neurol Sci 1981;51:141–55.

[5] Nishino I, Noguchi S, Murayama K, et al. Distal myopathy with rimmed vacuoles is allelic to hereditary inclusion body myopathy. Neurology 2002;59:1689–93.

[6] Tomimitsu H, Ishikawa K, Shimizu J, et al. Distal myopathy with rimmed vacuoles: novel mutations in the *GNE* gene. Neurology 2002;59:451–4.

[7] Tomimitsu H, Shimizu J, Ishikawa K, et al. Distal myopathy with rimmed vacuoles (DMRV): new *GNE* mutations and splice variant. Neurology 2004;62:1607–10.

[8] Izumi R, Niihori T, Aoki Y, et al. Exome sequencing identifies a novel TTN mutation in a family with hereditary myopathy with early respiratory failure. J Hum Genet 2013;58:259–66.

[9] Balduini CL, Savoia A. Genetics of familial forms of thrombocytopenia. Hum Genet 2012;131:1821–32.

[10] Nurden P, Debili N, Coupry I, et al. Thrombocytopenia resulting from mutations in filamin A can be expressed as an isolated syndrome. Blood 2011;118:5928–37.

[11] Malicdan MC, Noguchi S, Nonaka I, Hayashi YK, Nishino I. A GNE knockout mouse expressing human V572L mutation develops

features similar to distal myopathy with rimmed vacuoles or hereditary inclusion body myopathy. Hum Mol Genet 2007;16:115–28.
[12] Noguchi S, Keira Y, Murayama K, et al. Reduction of UDP-N-acetylglucosamine 2-epimerase/N-acetylmannosamine kinase activity and sialylation in distal myopathy with rimmed vacuoles. J Biol Chem 2004;279:11402–7.
[13] Greenberg J, Packham MA, Cazenave JP, Reimers HJ, Mustard JF. Effects on platelet function of removal of platelet sialic acid by neuraminidase. Lab Invest 1975;32:476–84.
[14] Kotze HF, van Wyk V, Badenhorst PN, et al. Influence of platelet membrane sialic acid and platelet-associated IgG on ageing and sequestration of blood platelets in baboons. Thromb Haemost 1993;70:676–80.
[15] Sorensen AL, Rumjantseva V, Nayeb-Hashemi S, et al. Role of sialic acid for platelet life span: exposure of beta-galactose results in the rapid clearance of platelets from the circulation by asialoglycoprotein receptor-expressing liver macrophages and hepatocytes. Blood 2009;114:1645–54.
[16] Tribulatti MV, Mucci J, Van Rooijen N, Leguizamon MS, Campetella O. The trans-sialidase from *Trypanosoma cruzi* induces thrombocytopenia during acute Chagas' disease by reducing the platelet sialic acid contents. Infect Immun 2005;73:201–7.
[17] Watanabe Y. The mechanism of the thrombocytopenia in patients with hepatic cirrhosis. J Jpn Soc Gastroenterol 1981;78:1216–25 (Japanese).
[18] Zhen C, Guo F, Fang X, Liu Y, Wang X. A family with distal myopathy with rimmed vacuoles associated with thrombocytopenia. Neurol Sci 2014.
[19] Kurochkina N, Yardeni T, Huizing M. Molecular modeling of the bifunctional enzyme UDP-GlcNAc 2-epimerase/ManNAc kinase and predictions of structural effects of mutations associated with HIBM and sialuria. Glycobiology 2010;20:322–37.
[20] Mori-Yoshimura M, Monma K, Suzuki N, et al. Heterozygous UDP-GlcNAc 2-epimerase and N-acetylmannosamine kinase domain mutations in the GNE gene result in a less severe GNE myopathy phenotype compared to homozygous N-acetylmannosamine kinase domain mutations. J Neurol Sci 2012;318:100–5.
[21] McMillan R. Autoantibodies and autoantigens in chronic immune thrombocytopenic purpura. Semin Hematol 2000;37:239–48.
[22] Ito M, Sugihara K, Asaka T, et al. Glycoprotein hyposialylation gives rise to a nephrotic-like syndrome that is prevented by sialic acid administration in GNE V572L point-mutant mice. PLoS One 2012;7:e29873.
[23] Galeano B, Klootwijk R, Manoli I, et al. Mutation in the key enzyme of sialic acid biosynthesis causes severe glomerular proteinuria and is rescued by N-acetylmannosamine. J Clin Invest 2007;117:1585–94.

Hum. Reprod. Advance Access published January 20, 2015
Human Reproduction, Vol.0, No.0 pp. 1–8, 2015
doi:10.1093/humrep/deu364

human reproduction ORIGINAL ARTICLE *Andrology*

Molecular basis of non-syndromic hypospadias: systematic mutation screening and genome-wide copy-number analysis of 62 patients

M. Kon[1,2], E. Suzuki[1], V.C. Dung[3], Y. Hasegawa[4], T. Mitsui[2], K. Muroya[5], K. Ueoka[6], N. Igarashi[7], K. Nagasaki[8], Y. Oto[9], T. Hamajima[10], K. Yoshino[11], M. Igarashi[1], Y. Kato-Fukui[1], K. Nakabayashi[12], K. Hayashi[12], K. Hata[12], Y. Matsubara[13], K. Moriya[2], T. Ogata[1,14], K. Nonomura[2], and M. Fukami[1,*]

[1]Department of Molecular Endocrinology, National Research Institute for Child Health and Development, Tokyo 157-8535, Japan [2]Department of Renal and Genitourinary Surgery, Hokkaido University Graduate School of Medicine, Sapporo 060-8638, Japan [3]Department of Endocrinology, The Vietnam National Hospital of Pediatrics, Hanoi, Vietnam [4]Department of Endocrinology and Metabolism, Tokyo Metropolitan Children's Medical Center, Tokyo 183-8561, Japan [5]Department of Endocrinology and Metabolism, Kanagawa Children's Medical Center, Yokohama 232-0066, Japan [6]Division of Urology, National Center for Child Health and Development, Tokyo 157-8535, Japan [7]Department of Pediatrics, Toyama Prefectural Central Hospital, Toyama 930-0975, Japan [8]Department of Pediatrics, Niigata University School of Medicine, Niigata 951-8510, Japan [9]Department of Pediatrics, Dokkyo Medical University Koshigaya Hospital, Koshigaya 343-0845, Japan [10]Division of Endocrinology and Metabolism, Aichi Children's Health and Medical Center, Obu 474-8710, Japan [11]Department of Urology, Aichi Children's Health and Medical Center, Obu 474-8710, Japan [12]Maternal-Fetal Biology, National Research Institute for Child Health and Development, Tokyo 157-8535, Japan [13]National Research Institute for Child Health and Development, Tokyo 157-8535, Japan [14]Department of Pediatrics, Hamamatsu University School of Medicine, Hamamatsu 431-3192, Japan

*Correspondence address. E-mail: fukami-m@ncchd.go.jp

Submitted on October 1, 2014; resubmitted on December 16, 2014; accepted on December 30, 2014

STUDY QUESTION: What percentage of cases with non-syndromic hypospadias can be ascribed to mutations in known causative/candidate/susceptibility genes or submicroscopic copy-number variations (CNVs) in the genome?

SUMMARY ANSWER: Monogenic and digenic mutations in known causative genes and cryptic CNVs account for >10% of cases with non-syndromic hypospadias. While known susceptibility polymorphisms appear to play a minor role in the development of this condition, further studies are required to validate this observation.

WHAT IS KNOWN ALREADY: Fifteen causative, three candidate, and 14 susceptible genes, and a few submicroscopic CNVs have been implicated in non-syndromic hypospadias.

STUDY DESIGN, SIZE, DURATION: Systematic mutation screening and genome-wide copy-number analysis of 62 patients.

PARTICIPANTS/MATERIALS, SETTING, METHODS: The study group consisted of 57 Japanese and five Vietnamese patients with non-syndromic hypospadias. Systematic mutation screening was performed for 25 known causative/candidate/susceptibility genes using a next-generation sequencer. Functional consequences of nucleotide alterations were assessed by *in silico* assays. The frequencies of polymorphisms in the patient group were compared with those in the male general population. CNVs were analyzed by array-based comparative genomic hybridization and characterized by fluorescence *in situ* hybridization.

MAIN RESULTS AND THE ROLE OF CHANCE: Seven of 62 patients with anterior or posterior hypospadias carried putative pathogenic mutations, such as hemizygous mutations in *AR*, a heterozygous mutation in *BNC2*, and homozygous mutations in *SRD5A2* and *HSD3B2*. Two of the seven patients had mutations in multiple genes. We did not find any rare polymorphisms that were abundant specifically in the patient group. One patient carried mosaic dicentric Y chromosome.

LIMITATIONS, REASONS FOR CAUTION: The patient group consisted solely of Japanese and Vietnamese individuals and clinical and hormonal information of the patients remained rather fragmentary. In addition, mutation analysis focused on protein-altering substitutions.

WIDER IMPLICATIONS OF THE FINDINGS: Our data provide evidence that pathogenic mutations can underlie both mild and severe hypospadias and that *HSD3B2* mutations cause non-syndromic hypospadias as a sole clinical manifestation. Most importantly, this is the first report documenting possible oligogenicity of non-syndromic hypospadias.

STUDY FUNDING/COMPETING INTERESTS: This study was funded by the Grant-in-Aid from the Ministry of Education, Culture, Sports, Science and Technology; by the Grant-in-Aid from the Japan Society for the Promotion of Science; by the Grants from the Ministry of Health, Labour and Welfare, from the National Center for Child Health and Development and from the Takeda Foundation. The authors have no competing interests to disclose.

TRIAL REGISTRATION NUMBER: Not applicable.

Key words: copy-number / hypospadias / mutation / polymorphism / susceptibility

Introduction

Hypospadias is a relatively common form of 46,XY disorders of sex development (DSD) observed in ~4–40 per 10 000 live births (Kurahashi *et al.*, 2004; Nassar *et al.*, 2007; Blaschko *et al.*, 2012). Hypospadias occurs either as an isolated anomaly or as a component of congenital malformation syndromes (Wu *et al.*, 2002; Kurahashi *et al.*, 2004). Although non-syndromic hypospadias is a multifactorial disorder induced by both genetic and environmental factors, this condition can also take place as a result of single gene mutations (Kurahashi *et al.*, 2004; Wang *et al.*, 2004; Chen *et al.*, 2007; Köhler *et al.*, 2009). Previous studies revealed familial aggregation of non-syndromic hypospadias (Schnack *et al.*, 2008; van Rooij et al., 2013). In most cases, familial hypospadias is equally transmitted from the paternal and maternal sides of the family and shows similar recurrence risks between the brothers and sons of patients, indicating a significant role of single gene mutations in the development of the disease (Schnack *et al.*, 2008).

In 2012, van der Zanden *et al.* (2012) reviewed 162 prior studies and listed 15 causative genes and three candidate genes for this condition. They also introduced 49 polymorphisms in 13 genes associated with disease risk, together with one susceptibility gene *CYP1A1* whose risk allele is yet to be determined. To date, however, there is no single report of systematic mutation analysis of the causative/candidate/susceptible genes. Likewise, while a small number of submicroscopic copy-number variations (CNVs) have been identified in patients with non-syndromic hypospadias (Tannour-Louet *et al.*, 2010), genome-wide copy-number analysis has been performed only in exceptional cases. Thus, the contribution of single gene mutations and submicroscopic CNVs to the etiology of non-syndromic hypospadias remains unknown.

The aim of this study was to clarify the frequency and type of genetic defects in patients with non-syndromic hypospadias. This study consisted of systematic mutation screening using next-generation sequencing (NGS) technology and cytogenetic analyses using comparative genomic hybridization (CGH) and fluorescence *in situ* hybridization (FISH).

Materials and Methods

Patients

A total of 57 Japanese and 5 Vietnamese patients with hypospadias participated in the study (Table I). All patients were referred to our clinics because of hypospadias. Patients with additional clinical features except for cryptorchidism and micropenis and those with cytogenetically detectable chromosomal abnormalities were excluded from this study. The 62 patients had no family history of 46,XY DSD. One of the 62 patients (case 18) was born to consanguineous parents. Hospital records of genital features at birth were obtained for 49 patients. Eleven patients manifested relatively mild hypospadias with the urethral opening at the anterior portion of the penis, while 14 and 24 patients presented with moderate (middle) and severe (posterior) hypospadias, respectively. Cryptorchidism and micropenis were observed in 5 and 11 patients, respectively.

Ethical approval

This study was approved by the Institutional Review Board Committee at the National Center for Child Health and Development and performed after obtaining written informed consent from the parents of patients.

Identification of nucleotide substitutions

Sequence analysis was carried out for 25 known causative/candidate/susceptible genes for non-syndromic hypospadias, i.e. *AR*, *ATF3*, *BMP4*, *BMP7*, *BNC2*, *CTGF*, *CYP1A1*, *CYR61*, *DGKK*, *EGF*, *ESR1*, *ESR2*, *FGF8*, *FGFR2*, *GSTM1*, *GSTT1*, *HOXA4*, *HOXB6*, *HSD3B2*, *HSD17B3*, *MAMLD1*, *MID1*, *NR5A1* (alias *SF1*), *SRD5A2*, and *WT1* (van der Zanden *et al.*, 2012). The coding regions of these genes were amplified from genomic DNA using the Haloplex Target Enrichment System (Design ID 02185-1348467147) (Agilent Technologies, Palo Alto, CA, USA), and were sequenced as 150 bp paired-end reads on a MiSeq sequencer (Illumina, San Diego, CA, USA). The average read depth of each amplicon was 115.0. Subsequently, nucleotide alterations in the samples were called by the Surecall system (Agilent Technologies) and SAMtools 0.1.17 software (http://samtools.sourceforge.net,12 January 2015, date last accessed) (Li *et al.*, 2009). In the present study, we focused on non-synonymous substitutions in the coding regions and nucleotide changes at splice sites. Substitutions detected by NGS were confirmed by Sanger direct sequencing. The primers utilized in the present study are available upon request.

Characterization of nucleotide substitutions

Functional consequences of nucleotide alterations were predicted by *in silico* analyses. Single nucleotide polymorphisms (SNPs) with allele frequencies of >1.0% in the general population (dbSNP, http://www.ncbi.nlm.nih.gov/,12 January 2015, date last accessed), except for those that have been reported as risk alleles (van der Zanden *et al.*, 2012), were excluded from further analyses. The effects of missense substitutions on protein function were predicted using Polyphen2 (http://genetics.bwh.harvard.edu/pph2/, 12 January 2015, date last accessed) (Adzhubei *et al.*, 2010), and those of intronic substitutions on splicing were assessed using Genome Project

Table I Nucleotide alterations identified in the present study.

Case[a]	Ethnic origin	Putative pathogenic mutation	Putative risk variant	Probable benign change	Copy-number alteration	Position of urethral opening[b]	Cryptorchidism	Micropenis
1	J	***AR* (p.S176R)**				Anterior	No	No
2	J	***AR* (p.A403V)**				No data	No data	No data
3	J	***AR* (p.R841S)**	*HSD17B3* (p.G289S)			Posterior	No	Yes
4	J	***AR* (delins[c])** *HOXB6* (p.S2N)	***MAMLD1* (p.N662S)**			No data	No data	No data
5	J	*BNC2* (p.M801R)				Posterior	No	No
6	V	***SRD5A2* (p.R227Q)[d]**	*HSD17B3* (p.G289S)			Posterior	No	Yes
7	V	***HSD3B2* (p.A10T)**	*SRD5A2* (p.R227Q)[d]			Posterior	Yes (right)	Yes
8	J		*HSD17B3* (p.G289S)	*CYP1A1* (p.T173R)	Y chromosome[e]	Posterior	No	No
9	J		***MAMLD1* (p.N662S)**			Anterior	No	No
10	J		*CYP1A1* (p.Q75P)			Middle	No data	No data
11	J		*CYP1A1* (p.A62P)			Middle	No	No
12	J		*BMP7* (p.T170M)			Middle	No	No
13	V		*HSD17B3* (p.G289S)			No data	No	No
14	J		*HSD17B3* (p.G289S)			Posterior	No	No
15	J		***HSD17B3* (p.G289S)**			Posterior	Yes	No
16	J		*HSD17B3* (p.G289S)			Posterior	No	No
17	J		*HSD17B3* (p.G289S)			Posterior	Yes (right)	Yes
18	J		*HSD17B3* (p.G289S)			Posterior	No	No
19	J		*HSD17B3* (p.G289S)			Middle	Yes (right)	Yes
20	J		*HSD17B3* (p.G289S)			Middle	No data	No data
21	J		***HSD17B3* (p.G289S)**			Middle	No	Yes
22	J		*HSD17B3* (p.G289S)			Anterior	No	No
23	J		***HSD17B3* (p.G289S)**			No data	No data	No data
24	J		*HSD17B3* (p.G289S)			No data	No data	No data
25	J		*HSD17B3* (p.G289S)			No data	No data	No data
26	J		*HSD17B3* (p.G289S) ***MAMLD1* (p.N662S)**			Middle	No	No
27	J		*HSD17B3* (p.G289S)	*BNC2* (p.M539V)		No data	No data	No data
28	J		*HSD17B3* (p.G289S)	*BNC2* (p.P614S)		No data	No data	No data
29	J		***MAMLD1* (p.N662S)**	*EGF* (p.S16R)		Posterior	No	No
30	J		*HSD17B3* (p.G289S)	*FGFR2* (p.M97V)		Anterior	No data	No data
31	J		*HSD17B3* (p.G289S)	*EGF* (p.S16R)		Middle	No	No
32	J		***MAMLD1* (p.N662S)**	*HSD3B2* (p.S284I) *EGF* (p.S16R)		Posterior	No	No

Continued

Table I *Continued*

Case[a]	Ethnic origin	Putative pathogenic mutation	Putative risk variant	Probable benign change	Copy-number alteration	Position of urethral opening[b]	Cryptorchidism	Micropenis
33	J		*HSD17B3* (p.G289S)	*HSD3B2* (p.R362W)		Anterior	No data	No data
34	J			*NR5A1* (g.IVS2-5G>A)		Posterior	No data	No data
35	J			*HOXB6* (p.P40S)		Posterior	No	Yes
36	J			***MAMLD1* (p.N675K)**		Posterior	No data	No data
37	J			*ESR2* (p.G67S)		Posterior	No	No
38	J			*EGF* (p.S16R) *BNC2* (p.I974V)		Middle	No data	No data

J: Japanese; V: Vietnamese.
Homozygous or hemizygous mutations/variations are boldfaced, and heterozygous substitutions are lightfaced.
[a]Cases 39–62 carried no nucleotide alterations in the target genes.
[b]Detailed clinical information was obtained only from 49 of the 62 patients.
[c]c.1995delTCAAGGCTATGAATGTCinsCAGAA; p.666delEGYECQinsRK.
[d]Homozygosity and heterozygosity of this mutation were described as a pathogenic defect and a disease-susceptible alteration, respectively.
[e]Copy-number gain of the region from Ypter to Yq11.223 and copy-number loss of the remaining Y chromosomal region.

Data (http://www.fruitfly.org/seq_tools/splice.html, 12 January 2015, date last accessed) (Reese *et al.*, 1997). Nucleotide deletions and insertions in the coding regions were assessed as 'probably damaging'.

Nucleotide alterations were classified into the following three groups: (i) putative pathogenic mutations: mutations that have been associated with 46,XY DSD or hitherto unreported nucleotide changes in causative genes that were assessed as 'probably damaging' or 'possibly damaging' by *in silico* analyses; (ii) putative risk variants: previously reported risk SNPs or novel substitutions in susceptibility genes, or rare SNPs in causative genes that were assessed as 'probably damaging' or 'possibly damaging'; and (iii) probable benign changes: nucleotide substitutions in causative/susceptible/candidate genes that were assessed as 'benign'. To determine the possible association between the SNPs (putative risk variants and probable benign changes) and disease risk, we compared allele frequencies in the patient group with those in the male general population. In the SNP analysis, we focused on Japanese patients, for whom the allele frequencies in the general population were available in the public database (dbSNP, http://www.ncbi.nlm.nih.gov/, 12 January 2015, date last accessed).

Statistical analysis

The statistical significance of the comparison of allele frequency in the patient group and the general population was evaluated using χ^2 and Fisher's exact probability tests.

Copy-number analyses

CNVs in the genome were screened by CGH using a catalog human array (8 × 60 k format, catalog number G4450A, Agilent Technologies), according to the manufacturers' instructions. In this study, we focused on copy-number alterations affecting genomic intervals larger than 1.5 Mb, which have a higher probability of being associated with disease phenotypes (Cooper *et al.*, 2011). We referred to the Database of Genomic Variants (http://projects.tcag.ca/variation/, 12 January 2015, date last accessed) to exclude known benign variants. Genomic structures of CNVs were characterized by FISH analysis.

Results

Identification and characterization of nucleotide substitutions

Eight putative pathogenic mutations were identified in seven patients (Table I and Fig. 1). The eight mutations consisted of three hemizygous missense mutations and one hemizygous deletion/insertion in *AR*, one heterozygous missense mutation in *HOXB6*, one heterozygous missense mutation in *BNC2*, and apparent homozygous mutations in *SRD5A2* and *HSD3B2*. Of these, the *AR* mutation in case 3 and the *SRD5A2* mutation in case 6 were previously identified in patients with 46,XY DSD (Melo *et al.*, 2003 in which the p.R841S mutation in *AR* was described as p.R840S; Sasaki *et al.*, 2003; van der Zanden *et al.*, 2012), while the other mutations were first identified in the present study.

Putative risk variants were identified in 30 patients (Table I and Supplementary Table SI). These variants included three known risk alleles for hypospadias and/or micropenis: rs2066476 in *HSD17B3*, rs2073043 in *MAMLD1* and rs9332964 in *SRD5A2* (Sasaki *et al.*, 2003; Fukami *et al.*, 2008; Sata *et al.*, 2010; Kalfa *et al.*, 2011; van der Zanden *et al.*, 2012). The SNPs in *HSD17B3* and *MAMLD1* were identified in the Japanese patient group and the male general population at similar frequencies. We also identified a rare SNP in the causative gene *CYP1A1* which was shared by the Japanese patients and the male

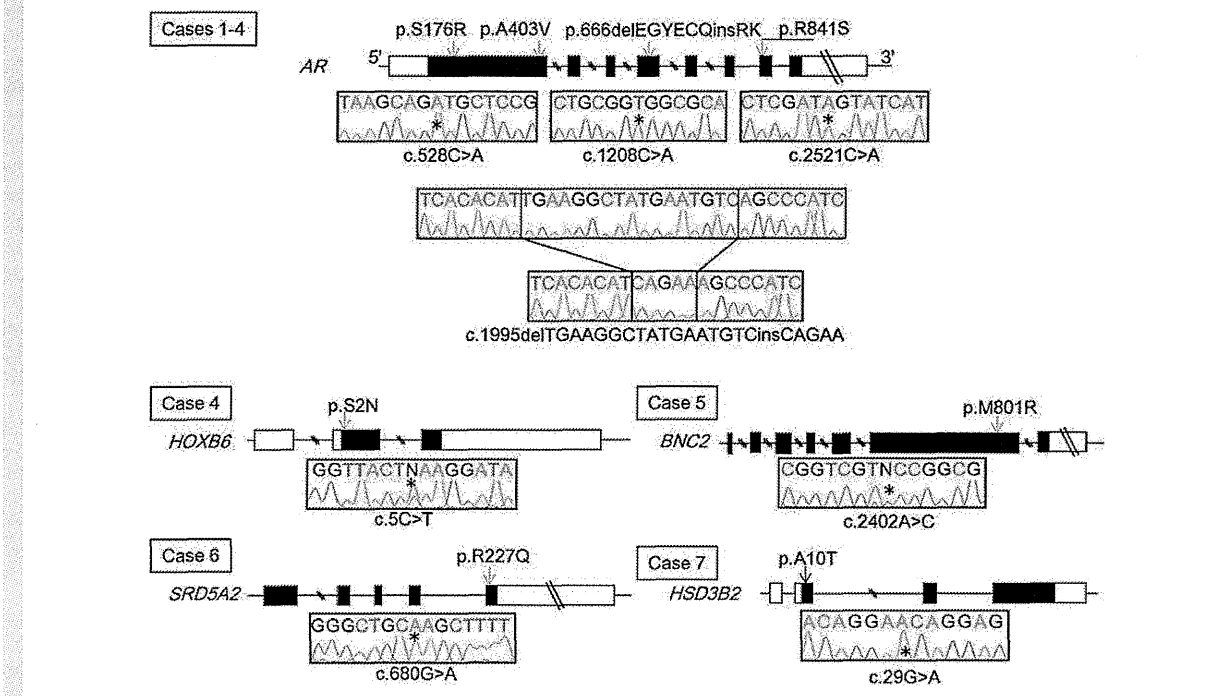

Figure 1 Putative pathogenic mutations identified in the present study. Genomic positions and chromatograms of the nucleotide substitutions are shown. Asterisks indicate the mutated nucleotides.

general population at a similar frequency, together with a SNP in *BMP4* whose frequency in the general population is unknown.

Probable benign changes were found in 13 patients (Table I and Supplementary Table SI). These substitutions included a rare SNP in *EGF* which was identified in the patient group and in the general population at similar frequency. We also detected SNPs in *ESR2* and *BNC2* that had unknown frequencies in the general population, together with a novel substitution in intron 2 of *NR5A1* (g.IVS2-5G>A) that was predicted to not affect splicing.

Copy-number analyses

One of the 62 patients (case 8) carried CNVs on the Y chromosome (Fig. 2A). These alterations consisted of copy-number gain of a ~23 Mb region from Ypter to Yq11.223 and copy-number loss of the remaining Y chromosomal region. The log2 signal ratios of most probes corresponding to the amplified and deleted regions were lower than +1.0 and higher than −2.0 respectively, indicating mosaicism of these CNVs. FISH analysis using a *SRY*-containing probe showed that case 8 had mosaic dicentric Y (Fig. 2B). CGH analysis for case 6 with an apparently homozygous *SRD5A2* mutation and case 7 with an apparently homozygous *HSD3B2* mutation excluded compound heterozygosity for a mutation and deletion (data not shown).

Clinical findings of patients with putative pathogenic defects

Putative pathogenic defects were associated with both anterior and posterior hypospadias (Table II). Endocrine evaluation of cases 1–8 remained fragmentary; blood hormone levels in cases 3 and 7 were within the normal range (Table II).

Discussion

Systematic mutation screening identified putative pathogenic mutations in 7 of 62 patients with non-syndromic hypospadias. These results, in conjunction with previous studies showing that ~30% of cases with severe hypospadias are ascribable to specific defects such as mutations in *AR* or *SRD5A2* (Albers *et al.*, 1997; Boehmer *et al.*, 2001), demonstrate the significant role of mutations in known causative genes in the etiology of non-syndromic hypospadias. Furthermore, our results support the previously proposed notion that genetic defects in *AR* account for a substantial percentage of cases with various types of 46,XY DSD (Albers *et al.*, 1997; Boehmer *et al.*, 2001; Audi *et al.*, 2010) and that mutations in *HSD3B2* can lead to non-syndromic hypospadias as a sole clinical manifestation, although *HSD3B2* plays an essential role in adrenal function (Boehmer *et al.*, 2001; Codner *et al.*, 2004; Audi *et al.*, 2010). Case 3 carried the p.R841S mutation in *AR*, which have been identified in patients with ambiguous genitalia (Melo *et al.*, 2003), suggesting the phenotypic diversity of missense mutations in *AR*. Notably, two of our patients had putative pathogenic mutations in multiple genes. Case 4 carried a hemizygous in-frame deletion/insertion in *AR* and a heterozygous missense substitution in *HOXB6*. Likewise, case 7 with a homozygous missense mutation in *HSD3B2* had an additional heterozygous missense mutation in *SRD5A2* that retains 3% of enzymatic activity (Makridakis *et al.*, 2000; Sasaki *et al.*, 2003). These data imply for the

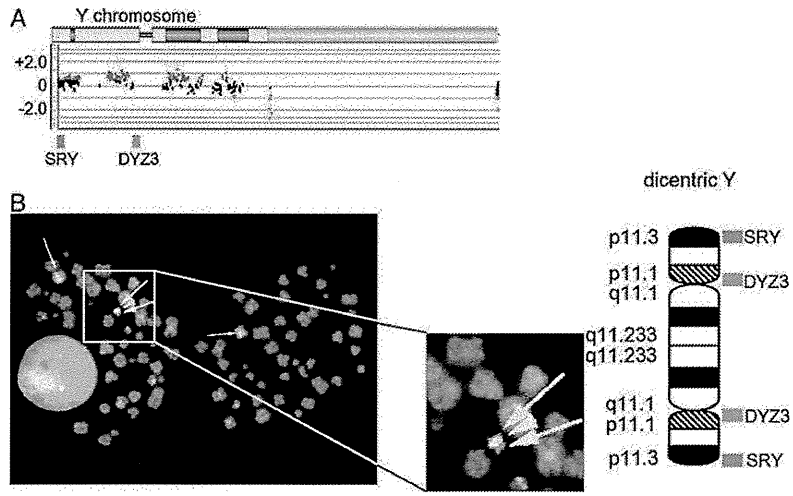

Figure 2 Copy-number alterations identified in case 8. Results of array-based comparative genomic hybridization (CGH) (**A**) and fluorescence *in situ* hybridization (FISH) analysis and schematic representation of the dicentric Y chromosome (**B**) are shown. The black, red and green dots in CGH denote signals indicative of the normal, increased ($>+0.4$) and decreased (<-0.8) copy-numbers, respectively. The arrowhead and thick arrows in FISH indicate a signal of DYZ3 (Y centromeric probe) and signals of *SRY*-containing probe (Yp11.3), respectively. The thin arrows in the left panel indicate signals of X centromeric probe.

Table II Molecular and clinical findings of patients with putative pathogenic abnormalities.

	Case 1	Case 2	Case 3	Case 4	Case 5	Case 6	Case 7	Case 8
Affected gene/region	*AR*	*AR*	*AR*	*AR/HOXB6*	*BNC2*	*SRD5A2*	*HSD3B2*	Y chromosome[a]
Ethnic origin	Japanese	Japanese	Japanese	Japanese	Japanese	Vietnamese	Vietnamese	Japanese
Family history of DSD	No	No data	No	No data	No	No	No	No
Clinical features								
Hypospadias[b]	Anterior	No data	Posterior	No data	Posterior	Posterior	Posterior	Posterior
Cryptorchidism	No	No data	No	No data	No	No	Yes (right)	No
Micropenis	No	No data	Yes	No data	No	Yes	Yes	No
Other features	No	No data	No	No data	No	No	No	Borderline MR
Endocrine findings								
Age at examination	No data	No data	15 months	No data	No data	No data	3.5 years	No data
LH (IU/l)[c]	No data	No data	<0.2 (<0.2–0.3)	No data	No data	No data	No data	No data
FSH (IU/l)[c]	No data	No data	<1.0 (<1.0–1.5)	No data	No data	No data	No data	No data
Testosterone (nmol/l)[c]	No data	No data	0.17 (0.10–0.45)	No data	No data	No data	0.16 (0.10–0.45)	No data

DSD, disorders of sex development; MR, mental retardation; LH, luteinizing hormone; FSH, follicle stimulating hormone.
[a]Copy-number alterations on Y chromosome.
[b]Position of urethral opening.
[c]Hormone values in parentheses indicate the reference ranges of age- and sex-matched control individuals.

first time that non-syndromic hypospadias results from digenic mutations. On the other hand, we did not observe the accumulation of rare SNPs in the patient group. Our data suggest that previously reported susceptibility SNPs play no or only minor roles in the development of non-syndromic hypospadias in the Japanese population. However, we cannot exclude the possibility that oligogenicity of these SNPs increases the risk of the disease, because a small number of our patients carried these SNPs as biallelic or digenic substitutions. Considering the small number of participants of this study, further investigations are necessary to clarify the possible association between rare SNPs and the disease phenotype.

Genome-wide copy-number analysis identified cryptic CNVs only in one patient. Case 8 carried a copy-number gain of a ~23 Mb region

on Yp and Yq and copy-number loss of the remaining Y chromosomal region. FISH analysis revealed that case 8 had mosaic dicentric Y, which has been described in multiple patients with hypospadias (Drummond-Borg *et al.*, 1988; Kojima *et al.*, 2001). It has been proposed that dicentric Y results in hypospadias by mosaic loss of the rearranged Y chromosome or by aberrant expression of Y chromosomal genes (Drummond-Borg *et al.*, 1988; Kojima *et al.*, 2001). The lack of pathogenic CNVs in the remaining 61 cases suggests the rarity of cryptic CNVs as genetic causes of non-syndromic hypospadias.

In this study, putative pathogenic defects were identified predominantly in patients with severe (posterior) hypospadias, while an *AR* mutation was detected in case 1, who manifested mild (anterior) hypospadias without micropenis or cryptorchidism. In this regard, previous studies have shown that syndromic hypospadias often arises from known gene mutations or chromosomal rearrangements (van der Zanden *et al.*, 2012). These data imply that monogenic mutations can underlie various types of hypospadias, although they are more strongly associated with severe or syndromic hypospadias than with mild non-syndromic hypospadias. Since identification of pathogenic defects can help to predict disease outcomes and improves the accuracy of genetic counseling, genetic analyses should be considered in patients with hypospadias of various clinical severities.

It should be pointed out that the present study has some limitations. First, the patient group consisted of only Japanese and Vietnamese individuals. Since the prevalence of hypospadias varies among countries (Nassar *et al.*, 2007; Serrano *et al.*, 2013), there may be ethnicity-specific causes of hypospadias. For example, mutations in *ATF3*, which account for ~10% of cases in the USA (Kalfa *et al.*, 2008), were absent from our cohort. In contrast, the p.A10T mutation in *HSD3B2* and the p.R227Q mutation in *SRD5A2* were detected exclusively in Vietnamese patients in homozygous state. Thus, our results are not simply applicable to other ethnic groups. Second, the frequency of monogenic defects may be underestimated in this study, because we focused on protein-altering mutations in 25 genes. Mutations/variations in regulatory regions, defects in unexamined genes and epigenetic abnormalities may be hidden in our mutation-negative patients. Lastly, clinical information of our patients remained fragmentary. Although previous studies have revealed that several factors such as low birthweight, placental insufficiency and maternal hypertension are associated with the risk of hypospadias (Stoll *et al.*, 1990; Weidner *et al.*, 1999; Fredell *et al.*, 2002; Brouwers *et al.*, 2010), the contributions of such factors to the disease phenotype of our patients are yet to be studied. Moreover, since endocrine data were unavailable for most of our mutation-positive cases, further studies are needed to elucidate the hormonal characteristics of each monogenic disorder.

Conclusion

The present study indicates that mutations in known causative genes and submicroscopic CNVs account for >10% of cases with non-syndromic hypospadias. Pathogenic defects appear to underlie both severe and mild hypospadias. On the other hand, previously reported risk SNPs are unlikely to play a major role in the development of the disease; further studies are required to validate this observation. Most importantly, this is the first report documenting the possible oligogenicity of non-syndromic hypospadias.

Supplementary data

Supplementary data are available at http://humrep.oxfordjournals.org/.

Authors' roles

M.K., K.No., T.O., and M.F. designed the study. M.K., E.S., V.C.D., Y.H., T.M., K.Mu., K.U., N.I., K.Nag., Y.O., T.H., K.Y., M.I, Y.K.-F., K.Nak., K.Hay., K.Hat., Y.M., K.Mo., and T.O. contributed to the acquisition of data. M.K. and M.F. analyzed data and wrote the paper. All authors were involved in revising the paper and approved the final version of the manuscript for submission.

Funding

This study was funded by the Grant-in-Aid from the Ministry of Education, Culture, Sports, Science and Technology; by the Grant-in-Aid from the Japan Society for the Promotion of Science; by the Grants from the Ministry of Health, Labour and Welfare, from the National Center for Child Health and Development and from the Takeda Foundation.

Conflict of interest

The authors declare that there is no conflict of interest.

References

Adzhubei IA, Schmidt S, Peshkin L, Ramensky VE, Gerasimova A, Bork P, Kondrashov AS, Sunyaev SR. A method and server for predicting damaging missense mutations. *Nat Methods* 2010;**7**:248–249.

Albers N, Ulrichs C, Glüer S, Hiort O, Sinnecker GH, Mildenberger H, Brodehl J. Etiologic classification of severe hypospadias: implications for prognosis and management. *J Pediatr* 1997;**131**:386–392.

Audi L, Fernández-Cancio M, Carrascosa A, Andaluz P, Torán N, Piró C, Vilaró E, Vicens-Calvet E, Gussinyé M, Albisu MA *et al.* Novel (60%) and recurrent (40%) androgen receptor gene mutations in a series of 59 patients with a 46,XY disorder of sex development. *J Clin Endocrinol Metab* 2010;**95**:1876–1888.

Blaschko SD, Cunha GR, Baskin LS. Molecular mechanisms of external genitalia development. *Differentiation* 2012;**84**:261–268.

Boehmer AL, Nijman RJ, Lammers BA, de Coninck SJ, Van Hemel JO, Themmen AP, Mureau MA, de Jong FH, Brinkmann AO, Niermeijer MF *et al.* Etiological studies of severe or familial hypospadias. *J Urol* 2001; **165**:1246–1254.

Brouwers MM, van der Zanden LF, de Gier RP, Barten EJ, Zielhuis GA, Feitz WF, Roeleveld N. Hypospadias: risk factor patterns and different phenotypes. *BJU Int* 2010;**105**:254–262.

Chen T, Li Q, Xu J, Ding K, Wang Y, Wang W, Li S, Shen Y. Mutation screening of BMP4, BMP7, HOXA4 and HOXB6 genes in Chinese patients with hypospadias. *Eur J Hum Genet* 2007;**15**:23–28.

Codner E, Okuma C, Iñiguez G, Boric MA, Avila A, Johnson MC, Cassorla FG. Molecular study of the 3 beta-hydroxysteroid dehydrogenase gene type II in patients with hypospadias. *J Clin Endocrinol Metab* 2004;**89**:957–964.

Cooper GM, Coe BP, Girirajan S, Rosenfeld JA, Vu TH, Baker C, Williams C, Stalker H, Hamid R, Hannig V *et al.* A copy number variation morbidity map of developmental delay. *Nat Genet* 2011;**43**:838–846.